Pacific Northwest
NATIONAL LABORATORY

PNNL-40193

Summary of Recent Phosphate-Based Waste Form Research for Electrorefiner Salt Wastes

December 2026

Brian J. Riley
Jonathan S. Evarts
Harmony S. Werth
Jincheng Bai
Yifeng Liao (ANL)

U.S. DEPARTMENT of ENERGY

Prepared for the U.S. Department of Energy
under Contract DE-AC05-76RL01830

DISCLAIMER

This report was prepared as an account of work sponsored by an agency of the United States Government. Neither the United States Government nor any agency thereof, nor Battelle Memorial Institute, nor any of their employees, makes **any warranty, express or implied, or assumes any legal liability or responsibility for the accuracy, completeness, or usefulness of any information, apparatus, product, or process disclosed, or represents that its use would not infringe privately owned rights**. Reference herein to any specific commercial product, process, or service by trade name, trademark, manufacturer, or otherwise does not necessarily constitute or imply its endorsement, recommendation, or favoring by the United States Government or any agency thereof, or Battelle Memorial Institute. The views and opinions of authors expressed herein do not necessarily state or reflect those of the United States Government or any agency thereof.

PACIFIC NORTHWEST NATIONAL LABORATORY
operated by
BATTELLE
for the
UNITED STATES DEPARTMENT OF ENERGY
under Contract DE-AC05-76RL01830

Printed in the United States of America

Available to DOE and DOE contractors from
the Office of Scientific and Technical Information,
P.O. Box 62, Oak Ridge, TN 37831-0062
www.osti.gov
ph: (865) 576-8401
fox: (865) 576-5728
email: reports@osti.gov

Available to the public from the National Technical Information Service
5301 Shawnee Rd., Alexandria, VA 22312
ph: (800) 553-NTIS (6847)
or (703) 605-6000
email: info@ntis.gov
Online ordering: http://www.ntis.gov

PNNL-40193

Summary of Recent Phosphate-Based Waste Form Research for Electrorefiner Salt Wastes

December 2026

Brian J. Riley
Jonathan S. Evarts
Harmony S. Werth
Jincheng Bai
Yifeng Liao (ANL)

Prepared for
the U.S. Department of Energy
under Contract DE-AC05-76RL01830

Pacific Northwest National Laboratory
Richland, Washington 99354

Executive Summary

The purpose of this report is to provide an overview of the phosphate-based waste form research conducted over the last six fiscal years (FY21 – FY26) between the Pacific Northwest National Laboratory and several collaborating institutions that include Argonne National Laboratory, Savannah River National Laboratory, University of Nevada Reno, University of North Texas, Missouri University of Science and Technology, Clemson University, Washington State University, Citrine Informatics, and MoSci Corporation to evaluate phosphate-based processes for treatment and immobilization of electrorefiner salt waste simulants. The current report provides updates to the Road Map Report (***Road Map for Developing Iron Phosphate Waste Forms for Salt Wastes***; PNNL-30998, ANL/CFCT-20/44) [1]. Specifically, details are provided for identified issues or gaps, summaries of the 36 publications (three from 2021, four from 2022, six from 2023, nine from 2024, eight from 2025, and six from 2026) and five additional related studies. The work documented a variety of waste simulants, glass-forming additives, salt loadings, and characterizations. The general categories of research that were identified as requiring additional study were *waste compositional variation studies*, *matrix/additive studies* (to improve properties), *waste processing studies*, *waste form performance studies*, *waste form property studies*, and *waste form acceptance studies*. Many of the issues identified and documented in the Road Map Report were addressed in the studies discussed within this report. The consensus from this work is that dechlorination can be performed on chloride salts using a variety of reagents [i.e., H_3PO_4, $NH_4H_2PO_4$, and $(NH_4)_2HPO_4$] whereby the decomposition byproducts are HCl, NH_4Cl, and/or H_2O. While the $40Fe_2O_3{\cdot}60P_2O_5$ (Fe:P = 0.667) composition shows promise as a foundational glass for salt immobilization, others show promise, including the DPF5 formulation (Fe:P = 0.655) as well as Fe_2O_3/Al_2O_3 mixtures as additives into P_2O_5. The main reason for ending this work is that an alternative dechlorination approach is showing promise and that is using organic acids instead of phosphates. The main drawback to using phosphate reagents for dechlorination reactions is that the phosphate remains within the glass melt following dechlorination, thereby diluting overall waste loading potential. The organic acid process allows for the organic acid anion (e.g., $C_2O_4^{2-}$) to decompose into carbonates and then oxides allowing for much higher salt cation loadings (< 2× higher) than the equivalent phosphate-based processes. Then, the full benefits are realized for organic-acid dechlorinated salts through utilization of the composition-property models for borosilicate glass waste forms, the most advanced nuclear waste form on the planet.

Acknowledgments

Pacific Northwest National Laboratory is operated by Battelle Memorial Institute for the U.S. Department of Energy (DOE) under Contract DE-AC05-76RL01830. The team acknowledges members of the various teams that contributed to this work and the work herein, including the following groups. Note that some of these are Nuclear Energy University Partnership (NEUP) projects along with a new Integrated Research Project (IRP; not included in this report) funded under DOE Office of Nuclear Energy (DOE-NE) with an August 2026 start date.

- Authors thank the Programmatic Support Team: **Zander Westesen** (PNNL) for his help as Project Manager as well as **Ken Marsden** (INL), **Kimberly Gray** (DOE-NE-43), and **Stuart Arm** (PNNL) for programmatic support under DOE-NE-43 leadership under the Material Recovery and Waste Form Development (MRWFD) Program.

- Authors thank the Rare-Earth Element Team: **Saehwa Chong**, **Mirka Peterson**, **Xiaonan Lu**, and **Zayne Nelson** of *PNNL*, **Jincheng Du** and **Mahadeva Sarma** of *University of North Texas* (UNT), and **Vinay Hegde** of *Citrine Informatics*.

- Authors thank the Advanced Research Projects Agency–Energy (ARPA-E) Optimizing Nuclear Waste and Advanced Reactor Disposal Systems (ONWARDS) Halogen-related Advanced Wasteforms through Artificial Intelligence Integration (HAWAII) Team, including **James Saal** (principal investigator, PI), **Kyle Miller**, and **Vinay Hegde** of *Citrine Informatics*; **Jincheng Du**, **Mahadeva Sarma**, and **Jayani Kalahe** of UNT and **John Vienna**, **Mirka Peterson**, **Xiaonan Lu**, and **Saehwa Chong** of *PNNL*.

- Authors thank additional staff from Argonne National Laboratory (ANL), including **Eva Schneiderlochner**, and **William Ebert** as well as past ANL employees **Sarah Stariha** and **J.A. Fortner**.

- Authors thank the Clemson University (CU) Team, including **Professor Kyle Brinkman** (PI), **Professor Ming Tang**, and **Peyton McGuire** under NEUP Project# CFA-21-24350, *Fabrication of Phosphate Ceramic Waste Forms for Advanced Immobilization of Chloride- and Fluoride-based Waste Streams*. Supporting collaborators on this project included **Professor John McCloy** (Washington State University or WSU), **S. Soudani** (WSU), **J. Bussey** (WSU), and **Jake Amoroso** (Savannah River National Laboratory or SRNL).

- Authors thank the University of Nevada Reno (UNR) Team, including **Professor Krista Carlson** (PI), **Paige Murray**, **Harmony Werth**, and **Jade Beland** and the Missouri University of Science and Technology (MUST) Team, including **Professor Charmayne Lonergan** (co-PI), **Professor Richard Brow**, **Lucas Greiner**, and **Kat Melenbrink** under NEUP contract# CFA-22-26614, *Investigation into the Processing Parameters of Phosphate-Based Dehalogenation for Chloride-Based Waste Salt*.

- Authors thank additional collaborators, including **CW Kim** (MoSci Corporation) as well as **John Vienna** (PNNL) and **José Marcial** (PNNL) and the rest of the contributors to the Phosphate Round Table Meeting held in 2020 with the full list provided elsewhere [1]. Authors also thank **Jarrod Crum** (PNNL) for helpful discussions throughout these projects.

This report was prepared as an account of work sponsored by an agency of the United States Government; here the Office of Materials and Chemical Technologies' MRWFD Program. Neither the United States Government nor any agency thereof, nor any of their employees, makes any warranty, express or implied, or assumes any legal liability or responsibility for the accuracy, completeness, or usefulness of any information, apparatus, product, or process disclosed, or represents that its use would not infringe privately owned rights. Reference herein to any specific commercial product, process, or service by trade name, trademark, manufacturer, or otherwise does not necessarily constitute or imply its endorsement, recommendation, or favoring by the United States Government or any agency thereof. The views and opinions of authors expressed herein do not necessarily state or reflect those of the United States Government or any agency thereof.

Acronyms and Abbreviations

ADP	ammonium dihydrogen phosphate ($NH_4H_2PO_4$)
AE	alkaline earth
AI	artificial intelligence
ANL	Argonne National Laboratory
ARPA-E	Advanced Research Projects Agency–Energy
ASTM	American Society for Testing and Materials International
BS	borosilicate (glass)
CCC	canister centerline cooling
CTE	coefficient(s) of thermal expansion
CU	Clemson University
DeVA	Dechlorination and Vitrification Apparatus
DHP	diammonium hydrogen phosphate [$(NH_4)_2HPO_4$]
DOE-NE	U.S. Department of Energy Office of Nuclear Energy
DP	dechlorinated product
DPF	dehalogenated phosphate forms
DPFR	DPF5-336 reference material
DPFR-I	intermediately cooled reference material
DPFR-M	moderately cooled reference material
DPFRQ	quenched DPF5 reference material
DPFSi	phosphosilicate glass made with silicate-doped DPF5-336 reference material
EBR-II	Experimental Breeder Reactor-II
ER	electrorefiner (salt)
FY	fiscal year
G2DA	Generation-2 Dechlorination Apparatus
GBS-CWF	glass-bonded sodalite ceramic waste form
HAWAII	Halogen-related Advanced Wasteforms through Artificial Intelligence Integration
HPLC	high-performance liquid chromatography
ICSD	Inorganic Crystal Structure Database
INL	Idaho National Laboratory
IRP	Integrated Research Project
LAW	low-activity waste
M	metal
MCC-1	Materials Characterization Center test number 1
MCFR	Molten Chloride Fast Reactor
ML	machine learning
MRWFD	Material Recovery and Waste Form Development (Program)

MSR	molten salt reactor
MUST	Missouri University of Science and Technology
NBS	sodium borosilicate (glass)
NEUP	Nuclear Energy University Partnership
NFP	sodium iron phosphate
NRC	Nuclear Regulatory Commission
OM	optical microscopy
ONWARDS	Optimizing Nuclear Waste and Advanced Reactor Disposal Systems
OR	oxide reduction (salt)
PCT	product consistency test
PI	principal investigator
PNNL	Pacific Northwest National Laboratory
RE	rare earth
SCC	slow cooling curve
SEM	scanning electron microscopy
SRNL	Savannah River National Laboratory
SRS	Savannah River Site
TEA	technoeconomic assessment
TGA	thermogravimetric analysis
UNF	used nuclear fuel
UNR	University of Nevada Reno
UNT	University of North Texas
VHT	vapor hydration test
WF	waste form
WL	waste loading
WSU	Washington State University
WTP	Hanford Waste Treatment and Immobilization Plant

Contents

Executive Summary ii
Acknowledgments iii
Acronyms and Abbreviations v
1.0 Introduction 1
2.0 Studies Performed Within the Timeframe of 2021 – 2026 3
2.1 Description of Recent Studies 3
2.1.1 Summary of Phosphate-Based Studies 3
2.1.2 Summary of Relevant and Related Studies Outside Phosphates 9
2.2 Summary of Salt Simulants Evaluated 10
2.3 Summary of the Glass Binders Evaluated 11
3.0 Updates to the Road Map 13
4.0 Comparisons between Options 18
5.0 Summary and Conclusions 19
6.0 Recommendations for Future Work 21
7.0 References 22
Appendix A – Additional Details about Recent Studies A1
Appendix B – Road Map Categories B2

Figures

Figure 1-1. Simplified diagram showing aspects of waste form development with emphasis on the preprocessing. 2
Figure 4-1. Summary of the calculated waste form volume (starting from 100 g salt) versus salt cation mass loading in various waste forms, including (a) several waste forms and (b) a magnified view of the organic acid dehalogenation samples resulting in borosilicate glass (BSG) waste forms; the phosphate waste forms are denoted in blue as P1, P2, P3, and DPF5-336. This figure was modified from previous versions by Riley [69] and Oshiro et al. [22] to include the new TARSv2 compositions. Note that part (a) is a semi-log plot. See text for descriptions of the other waste forms. This figure comes from Oshiro et al. [63]. 18

Tables

Table 2-1. Summary of salt simulant compositions (mass%) utilized in phosphate-based work in recent years. See the text above for example studies in which these salts were used. 11
Table 2-2. Summary of silicate glass binder compositions (mass%), including composition (if known), processing temperature used to vitrify the glass, the bulk density (ρ_b), glass transition temperature (T_g), softening point (T_s), the coefficient of thermal expansion (CTE) at two different

temperature ranges, and references for studies where these glasses were utilized. Standard deviations are provided for some of the values where available. These values come from Riley et al. [5] and from the 7056 Technical Data Sheet from Corning [67]. 12

Table 3-1. Summary of **Waste Composition** issues identified, approaches to fill gaps, and updates since the Road Map [1] was written in 2021. See Table B-1 (Appendix B) for the original list. 13

Table 3-2. Summary of **Matrix and Additives** issues identified, approaches to fill gaps, and updates since the Road Map [1] was written in 2021. See Table B-2 (Appendix B) for the original list. 14

Table 3-3. Summary of **Waste Processing** issues identified, approaches to fill gaps, and updates since the Road Map [1] was written in 2021. See Table B-3 (Appendix B) for the original list. 15

Table 3-4. Summary of **Waste Form Properties** issues identified, approaches to fill gaps, and updates since the Road Map [1] was written in 2021. See Table B-4 (Appendix B) for the original list. 16

Table 3-5. Summary of **Waste Form Acceptance** issues identified, approaches to fill gaps, and updates since the Road Map [1] was written in 2021. See Table B-5 (Appendix B) for the original list. 17

Table 3-6. Summary of **Waste Form Performance** issues identified, approaches to fill gaps, and updates since the Road Map [1] was written in 2021. See Table B-6 (Appendix B) for the original list. 17

1.0 Introduction

The baseline waste form process under the U.S. Department of Energy Office of Nuclear Energy (DOE-NE) for immobilizing used electrorefiner (ER) salt from electrochemical processing of Experimental Breeder Reactor-II (EBR-II) fast reactor fuel is the glass-bonded sodalite ceramic waste form (GBS-CWF) [2-4]. In this process, used salt is mixed with zeolite 4A to occlude the salt within the zeolite pores at 500°C, the salt-occluded zeolite is mixed with a glass binder and then heated to 925°C under pressureless sintering to convert the product to glass-bonded sodalite [i.e., $Na_8(AlSiO_4)_6Cl_2$] [2, 5]. While this process works for this waste, the waste loading limits are low (≈ 8 mass%) before residual halite (NaCl) starts to form with larger salt loadings [5]. Due to the low loading in this waste form system, additional work has been ongoing within the Material Recovery and Waste Form Development (MRWFD) Program.

Different processes being considered include simplified ways to produce the GBS-CWF and other waste forms, i.e., tellurite glass and dehalogenated salt waste forms (e.g., phosphate, borosilicates). Two primary options are being explored for simplified ways to produce GBS-CWF. First, ANL and the Idaho National Laboratory (INL) are evaluating use of larger sizes of zeolite, salt, and glass and ways for shortening the heat-treatment times and lowering the heat treatment temperature [6]. The main benefits are faster processing and reduction of fine particles. Second, salt bring loading into zeolite is being evaluated at INL instead of dry salt occlusion [7]. The goals of this are to improve homogeneity of the salt incorporation into zeolite for sodalite production but can also be used to load ER salt into zeolite for storage to reduce moisture absorption from air due to the hygroscopicity of high-LiCl salts.

Other waste forms being explored include using a glass system for direct salt immobilization [8-11]. The main glass system being explored include heavy-metal oxide glass systems, e.g., tellurite glass, but the chemical durabilities of these glasses vary extensively and are often below the performance of GBS-CWF. It is possible that the simplified processing route of direct vitrification will bump these glasses options above GBS-CWF, but that remains to be seen. Second, dehalogenation (halide removal) salt partitioning processes are being evaluated to simplify the residual waste (including fission products) because, by removing the Cl, which limits waste loading in all waste form options, the salt cation loadings can be notably increased. Products from phosphate-based dehalogenation can be immobilized in iron phosphate glass-ceramic waste forms [12-18] or iron phosphosilicate waste forms [19, 20]. Products from organic-acid-based dehalogenation can be immobilized in a borosilicate glass-ceramic waste form [21, 22].

The purposes of this report are to (a) provide a status update on the phosphate-based work as it has officially put on hold at this point in time within the MRWFD Program, (b) provide an overview of the most impactful findings from the recent work, and (c) set a path forward for suggested future work if this scope were to be reinitiated in the future (i.e., an updated road map). In general, the six categories identified within the Road Map [1] that required additional study include: *Waste Composition*, *Matrix and Additives*, *Waste Processing*, *Waste Form Properties*, *Waste Form Acceptance*, and *Waste Form Performance*, which are all shown schematically within Figure 1-1.

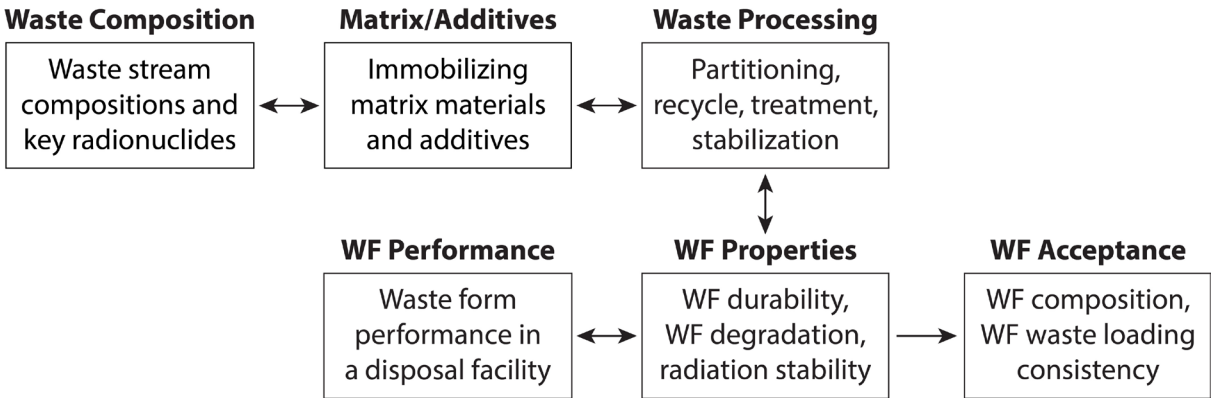

Figure 1-1. Simplified diagram showing aspects of waste form development with emphasis on the preprocessing.

For reference, the general formulas for dechlorination of salt streams using ADP and H_3PO_4 are shown below in Equations (1) – (3) and Equations (4) – (6), respectively, for metal chlorides (MCl_x) of different oxidation states, i.e., M^+, M^{2+}, M^{3+}. For ADP-based dechlorination reactions, the expected chloride byproduct is NH_4Cl, which can reversibly thermally decompose into $NH_3(g)$ and $HCl(g,l)$ – see Equation (7). For the H_3PO_4-based reactions, the chloride byproduct is $HCl(g,l)$. In all reactions, the off-gas stream will also contain H_2O.

$$2\ NH_4H_2PO_4(s) + 2\ MCl(s) \rightarrow M_2O{\bullet}P_2O_5\ (glass) + 2\ NH_4Cl(g,s) + 2\ H_2O(g) \quad (1)$$

$$2\ NH_4H_2PO_4(s) + MCl_2(s) \rightarrow MO{\bullet}P_2O_5\ (glass) + 2\ NH_4Cl(g,s) + 2\ H_2O(g) \quad (2)$$

$$6\ NH_4H_2PO_4(s) + 2\ MCl_3(s) \rightarrow M_2O_3{\bullet}3\ P_2O_5\ (glass) + 6\ NH_4Cl(g,s) + 6\ H_2O(g) \quad (3)$$

$$2\ H_3PO_4(l) + 2\ MCl(s) \rightarrow M_2O{\bullet}P_2O_5\ (glass) + 2\ HCl(g,l) + 2\ H_2O(g) \quad (4)$$

$$2\ H_3PO_4(l) + MCl_2(s) \rightarrow MO{\bullet}P_2O_5\ (glass) + 2\ HCl(g,l) + 2\ H_2O(g) \quad (5)$$

$$6\ H_3PO_4(l) + 2\ MCl_3(s) \rightarrow M_2O_3{\bullet}3\ P_2O_5\ (glass) + 6\ HCl(g,l) + 6\ H_2O(g) \quad (6)$$

$$NH_4Cl(g,s) \rightarrow NH_3(g) + HCl(g,l)\ [T \geq 200°C] \quad (7)$$

2.0 Studies Performed Within the Timeframe of 2021 – 2026

2.1 Description of Recent Studies

Below is a list of studies and documents published on the topic of phosphate-based waste form development (and related research) along with brief descriptions by the national laboratory team (i.e., PNNL, ANL) and associated university collaborators [e.g., University of Nevada Reno (UNR), Missouri University of Science and Technology (MUST), Clemson University (CU)] that overlap across relevant categories. While most of this work was done under funding from DOE-NE, related work was done under ARPA-E (Advanced Research Projects Agency–Energy) ONWARDS (Optimizing Nuclear Waste and Advanced Reactor Disposal Systems) Project "HAWAII" (Halogen-related Advanced Wasteforms through Artificial Intelligence Integration) and is also listed here because these additional studies provide supporting data and information. Typically, waste forms were characterized using similar processes, including optical microscopy (OM), X-ray diffraction (XRD), scanning electron microscopy (SEM), energy dispersive X-ray spectroscopy (EDS), and chemical durability analysis with internationally approved procedures from the American Society for Testing and Materials International (ASTM), e.g., ASTM C1220 (referred to as Materials Characterization Center test number 1 or MCC-1) [23], ASTM C1285 (product consistency test or PCT) [24], ASTM C1308 [25], and ASTM C1663 (vapor hydration test or VHT) [26]. Some tests refer to the DPF5-336 reference material (also referred to as DPFR),[a] documented elsewhere in more detail [27], which is an iron phosphate glass made with the DPF-5 composition (i.e., Fe:P = 0.655 mole ratio, P:alkali = 1.639 mole ratio) [14] whereby oxides of salt cations from the salt waste represent a mole fraction of 0.336 [27]. Additional Details are provided for the salt simulants in Section 2.2 and for the glass binders used in Section 2.3.

2.1.1 Summary of Phosphate-Based Studies

#1 (2021) "***Crystalline compounds for remediation of rare-earth fission products: A review***," by Chong et al. [28]. This paper summarizes a range of different crystalline compounds that can be used to immobilize rare earth fission products. The full list of crystal families explored in this work included oxyapatite [$AE_2RE_8(SiO_4)_6O_2$], oxychloride (REOCl), borosilicate ($RE_3BSi_2O_{10}$), pyrochlore ($RE_2M_2O_7$), monazite ($REPO_4$), and perovskite ($REMO_3$) where AE denotes alkaline earth metals, M denotes transition metals, and RE denotes rare earths. Details in the paper include synthesis methods for making these crystalline compounds along with the crystallography and summaries of various chemistries provided within the Inorganic Crystal Structure Database (ICSD) for these crystal families.

#2 (2021) "***Dechlorination Apparatus for Treating Chloride Salt Wastes: System Evaluation and Scale-Up***," by Riley et al. [15]. This paper summarizes a dechlorination study done on single-salt additives (i.e., KCl, CsCl) in a new "Generation-2 Dechlorination Apparatus" (G2DA) built at PNNL using a custom-built five-zone gradient furnace. With these single salt reagents, the dechlorination efficiencies were 83.4% for KCl and 85.5% for CsCl.

#3 (2021) "***Corrosion Behavior of Developmental Iron Phosphate Waste Forms: FY21 Status Report***," by Stariha et al. [29]. This report summarizes chemical durability testing performed on DPF5-336 (reference material) CCC treated in fused quartz and alumina crucibles along with the simplified DPF5 and compositions and DPF5 compositions produced with KCl, $SrCl_2$, CsCl, or LiCl. Durability testing results showed that the Li and K retention were lower and Cs retention in the CCC-treated materials were only slightly lower than quenched materials.

[a] DPF5-336 has a target dechlorination starting point of DP:Fe_2O_3 = 1.9307 (g/g) for ERV3 salt.

#4 (2022) "***Effects of Composition and Canister Centerline Cooling on Microstructure, Phase Distribution, and Chemical Durability of Dehalogenated Iron Phosphate Waste Forms***," by Riley and Chong [30]. This paper summarizes a series of experiments performed to assess dechlorination with ADP and different salt constituents, i.e., LiCl, KCl, CsCl, $SrCl_2$, $LaCl_3$, $NdCl_3$, or ERV2 at the same mass ratios of ADP:salt:Fe_2O_3. Dechlorination was performed at the same conditions for each experiment (5°C/min ramp rates with 1-hr dwells at 200, 300, 400, and 600°C utilizing the G2DA at PNNL. Following dechlorination, the products were vitrified with Fe_2O_3 additions in separate crucibles at different temperatures of 1050°C [LiCl (60 min), KCl (90 min), $SrCl_2$ (90 min), and ERV2 (60 min)], 1100°C [CsCl (90 min)], or 1350°C [$LaCl_3$ (92 min) and $NdCl_3$ (90 min)] followed by a canister centerline cooling (CCC) profile (see Figure A-2) to simulate the slow cooling rate of a larger-scale test run. Notable amounts of alumina were found in the vitrified glasses. Also, during the vitrification and CCC steps, most samples showed evidence of volatilization during the process. One major takeaway from this study was that many of the issues that arose during the study with volatility, crucible reactions, and/or unreacted (or high-melting) constituents might be solved by adding the single salt components into the LiCl-KCl eutectic to lower the melting temperature.

#5 (2022) "***Conceptual Iron Phosphate Waste Form Degradation Model***," by Ebert [31]. This report summarizes the conceptional degradation model for iron phosphate waste form performance. Some key notes documented in this report include (a) "..in terms of the reaction affinity, the assemblage of phosphate-bearing phases within the waste form will establish a phosphate solubility limit when first contacted by seepage water…," (b) "…although the phase assemblage will likely evolve over time as the waste form degrades, the system energetics will likely remain nearly constant because new phases will not be significantly more stable than the primary phases…," and (c) "…the same model and test methods developed for borosilicate waste glasses are appropriate for iron phosphate waste forms because the iron phosphate glass phase that hosts the majority of waste constituents degrades by the same mechanism as borosilicate waste glasses and the primary crystalline phases formed in DPF materials serve the same role as precipitated secondary phases in long-term borosilicate glass corrosion…"

#6 (2022) "***Corrosion Behavior of Fast-Cooled Iron Phosphate Reference Material***," by Stariha et al. [32]. This report summarizes extensive chemical durability testing (ASTM C1285, C1220, C1308, and C1663) on quenched DPF5 reference material (called DPFRQ) made at PNNL. The dissolution behaviors observed for these materials were reported as being like those of borosilicate waste glass materials where the degradation mechanism is "…dominated by a surface dissolution process and the kinetics are attenuated by solution feedback effects (reaction affinity), although the effective solubility remains to be measured…"

#7 (2022) "***Dehalogenation Reactions Between Halide Salts and Phosphate Compounds***," by Riley and Chong [33]. This paper describes unwanted compounds, with some being very hazardous (and even considered contact explosives), that can form between nitrogen-containing reagents and halide salts at elevated temperatures, e.g., NCl_3, NBr_3, NI_3, NH_4I_3. This study prompted the research group to remove iodine from the salt simulants (i.e., ERV2 → ERV3).

#8 (2023) "***Crystalline Versus Glassy Nature of Iron Phosphate Waste Forms Subjected to Different Slow Cooling Curves***," by Riley et al. [34]. This report summarizes a range of DPF5-336 materials made under different slow cooling curves (SCC), labeled as SCC#2, SCC#3, or SCC#5 (see Figure A-3, Appendix A), followed by material characterizations. For details on what these curves are, SCC#1 was the fastest cool (not evaluated, but theoretical), SCC#2 was a furnace cool, SCC#3 was an intermediate cool, SCC#4 was a CCC cool (see Figure A-1 [35]) not tested in this study but was in other studies documented herein [36], and SCC#5 was the slowest cooling rate. The SCC#1 (*fastest cool*) rate was derived from a fast-cooling profile of a 4"-diameter crucible from 1200°C based on modeling done by collaborators (M. Kesterson and J.

Amoroso) at Savannah River National Laboratory (SRNL) and Savannah River Site (SRS) [37]. The SCC#2 (*furnace cool*) rate is the fastest possible curve achieved when turning off a high-temperature Deltech furnace at 1200°C and allowing it to cool to ambient temperature. The SCC#3 (*intermediate cool*) was a cool-down from 1200°C to room temperature using a linear cooling rate of -0.7542°C/min. The SCC#4 (*CCC cool*) is based off the CCC curve for Hanford high-level waste (HLW) glasses tested at the Hanford Waste Treatment and Immobilization Plant (WTP) with a starting cool-down temperature of 1050°C [38]; this curve has been run in previous experiments [30, 36]. Finally, the SCC#5 (*slowest cool*) is an intermediate cool from 1200°C to room temperature using a linear cooling rate of -0.3904°C/min. Crystal fractions across the SCC#2, SCC#3, and SCC#5 samples were all similar ranging in crystal content of 35.66–41.14 mass% split across up to ≈ 10 different crystalline phase in each sample (i.e., phase distribution was complicated). Microstructural analysis from SEM is provided in Figure A-4 (Appendix A). Data presented in an ANL report [39] is discussed below.

#9 (2023) "***Canister Centerline Cooling Experiments for DPF5-336 Reference Material Made with ERV3b Salt Simulant***," by Riley et al. [36]. This report summarizes experiments done to dechlorinate ERV3b salt simulant with ADP (to an efficiency of 92 mass%) and vitrify the glass. Following vitrification, the glass was then placed in fused quartz and alumina crucibles to reheat and then CCC treat. The products were mounted in epoxy and polished for SEM and optical microscopy (see Figure A-5, Appendix A). Portions were analyzed with XRD. Microstructural characterizations were complicated. Data presented in an ANL report [39] on these samples showed that the durability of the materials CCC cooled in the fused quartz crucibles outperformed those slow cooled in the alumina crucibles.

#10 (2023) "***Aluminophosphate Waste Forms for Immobilizing Cations from Electrochemical Salt Wastes***," by Riley et al. [40]. This report summarizes work done to evaluate aluminophosphate matrices as replacements for iron-phosphate matrices. The main driver for this work was due to the inherent Al_2O_3 contamination from alumina crucible dissolution for ADP-driven dechlorination and vitrification. For this work, three new samples were made and compared with the DPF5-336 reference composition [27]. First, two samples were made using 50/50 exchange of Al_2O_3 in place of Fe_2O_3 on either a mass basis or a mole basis. Then, a third sample was produced with no Fe_2O_3. Pictures of these four glasses are shown in Figure A-6 (Appendix A). Data presented in an ANL report [39] on these samples showed that durability improvements were made to the DPF5-336 reference material with 50/50 alumina substitutions (i.e., G3 on mass basis, G5 on molar basis) but the glass made without Fe_2O_3 (i.e., G6) was not nearly as durable as any of the three other glasses tested in this set.

#11 (2023) "***Conceptual Design of a Salt Dechlorination and Vitrification Apparatus (DeVA)***," by Tolman and Riley [41]. This report summarizes an apparatus designed in collaboration between INL and PNNL for incorporation of phosphate-based dechlorination within a hot cell that could be used to convert U^0 dendrites into UCl_x in situ using the NH_4Cl produced from the dechlorination reaction. The conceptual process and instrumentation diagram along with the conceptual model are shown in Figure A-7 (Appendix A).

#12 (2023) "***Durability Assessments of Quenched and Slow-Cooled Iron Phosphate Waste Form Materials***," by Stariha et al. [39]. This report summarizes chemical durability testing results on the samples described above from the Riley et al. [34] study. Samples were studied using ASTM C1220, ASTM C1285, ASTM C1308, and ASTM C1663 experiments. Results showed that Cs-containing crystalline materials were not as durable as desired based on incongruent alkali release rates. Comparisons were made between quenched DPF5-336, CCC-treated DPF5-336, iron-aluminophosphate glass (G3, G5), and an aluminophosphate glass (G6) (see Figure A-8, Appendix A). A conclusion from this study was that additional additives, such as borosilicate glass that would not interact with the phosphate glass or phosphate-based crystalline phases that could

form during slow cooling, might help in devitrification and this led to additional studies by Evarts et al. [19, 20] described below.

#13 (2023) "***Corrosion Tests with Phosphate-Based Materials Made at Clemson University***," by Stariha et al. [42]. This report summarizes ASTM C1308 testing results on different sets of glasses, including set-1 named CU1-1–CU1-9 made with P_2O_5 and different additives (i.e., Fe_2O_3, Fe_3O_4, SnF_2), plus a LiCl-10Li_2O-20SrO and set-2 named CU2-1–CU2-16 made with ADP or P_2O_5 and Fe_2O_3 or $FePO_4$ plus BaO (as waste). Additions of SnF_2 and BaO were detrimental to the chemical durability of those compositions containing that additive whereas Fe_2O_3 and Fe_3O_4 revealed improvements in chemical durability.

#14 (2024) "***Phosphate-Based Dechlorination of Electrorefiner Salt Waste Using a Phosphoric Acid Precursor***," by Murray et al. [16]. This paper summarizes a dechlorination study performed with a simplified salt composition (48LiCl-33KCl-19NaCl mol%) with H_3PO_4 as the dechlorination reagent within both air and argon atmospheres. The main takeaway from this study is that dechlorination was performed at lower temperature in air than in argon. Another observation was the high corrosivity of the off-gas, which contained HCl, coming off the off-gas line and the 304 stainless-steel flanges on ends of the tube furnace.

#15 (2024) "***Bonding Environments and Radiation Stabilities of Phosphate Glasses***," by Marcial et al. [43]. This report summarizes the key discussion points presented by attendees at the Phosphate Round Table Workshop held jointly with PNNL and ANL in August 2020. At a high level, topics covered within this report include discussion of the history of phosphate glass research for waste forms within the world, phosphate glass structure-property relationships, and phosphate glass radiation tolerance.

#16 (2024) "***Insights on the Structure and Properties of Sodium Iron Phosphate Glasses from Molecular Dynamics Simulations***," by Kalahe et al. [44]. This paper (done under ARPA-E ONWARDS Project "HAWAII") summarizes molecular dynamics simulation results, using effective two-body and three-body potentials, for three series of sodium iron phosphate (NFP) glasses, including 60P_2O_5-(40-x)Fe_2O_3-$x$$Na_2O$ (x = 0→40), (100–2x) P_2O_5-$x$$Fe_2O_3$-$x$$Na_2O$ (x = 5→17.5) and one with a different iron redox ratio, to understand the composition as well as the iron redox effects on the structure and properties of these glasses. The calculated bond lengths and coordination numbers were consistent with reported experimental values.

#17 (2024) "***Towards Informatics-Driven Design of Novel Nuclear Waste Forms***," by Hegde et al. [45]. This paper (done under ARPA-E ONWARDS Project "HAWAII") summarizes the machine learning and artificial intelligence (ML/AI) approach used to develop next-generation iron phosphate waste form compositions. The approach is shown schematically in Figure A-9 (Appendix A). The proposed data-driven methodology optimally leverages physics-based simulations, experimental synthesis/characterization, and ML surrogates.

#18 (2024) "***Structure and structure-property relationship in sodium iron phosphate glasses from Molecular Dynamics Simulations and QSPR analysis***," by Du et al. [46]. This paper (done under ARPA-E ONWARDS Project "HAWAII"), summarizes molecular dynamics simulations, performed with effective partial charge potentials, on two separate NFP glass series, i.e., 70P_2O_5-(30-x)Fe_2O_3-$x$$Na_2O$ (x = 0, 5→30) [P70_series] and (100-x)[0.7P_2O_5-0.3Fe_2O_3]-$x$$Na_2O$ (x = 5→20); P:Fe=7:3 [P/Fe = 7/3 series].

#19 (2024) "***Synthesis and Properties of Anhydrous Rare-Earth Phosphates, Monazite and Xenotime: A Review***," by Chong et al. [47]. This paper summarizes a range of properties of monazite (*RE* = La → Gd) and xenotime (*RE* = Gd → Lu, Y) compounds (see Figure A-10, Appendix A), including synthesis methods, crystal structures, properties (i.e., mechanical, thermal, radiation stability, optical), and the applications of interest for these compounds.

#20 (2024) "***Compositional effects on the chemical durabilities of aluminophosphate glasses: A review***," by Chong and Riley [48]. This paper summarizes studies found in literature where chemical durability tests were run on aluminophosphate glasses. The extended variety of different test conditions makes an exact comparison between results challenging where dissolution rates (converted to $g/m^2/d$) ranged by nearly 14 orders of magnitude on a $\log_{10}$ scale. A takeaway from this paper is that the addition of Al_2O_3 generally improves chemical durability in alkali oxide-containing glasses (see Figure A-11, Appendix A).

#21 (2024) "***Completion of Milestone M4FT-24PN030104046 "Support ANL-led efforts towards dechlorinated waste forms***," by Evarts and Riley [49]. This milestone memo discusses a series of phosphosilicate glasses, which were based on the DPF5-336 (reference iron phosphate material) composition, but loaded with 0, 2.5, 5, 10, 15, or 30 mass% of NBS-3 glass binder added within the crucible before the during the vitrification of dechlorinated product (DP) and Fe_2O_3 followed by slow-cooling step.

#22 (2024) "***Effect of Added Borosilicate Glass on Iron Phosphate Waste Form Material Durability***," by Ebert et al. [50]. This report summarizes chemical durability tests run on a series of phosphosilicate glasses, which were based on the DPF5-336 (reference iron phosphate material) composition, but loaded with 0, 2.5, 5, 10, 15, or 30 mass% of NBS-3 glass binder added within the crucible before the during the vitrification of DP and Fe_2O_3 followed by slow-cooling step; more details on these samples are provided elsewhere [19, 49]. The main takeaway from this study was that the 5 mass% NBS-3 sample showed the biggest improvement over the DPF5-336 composition made without NBS-3 (see Figure A-12; Appendix A).

#23 (2025) "***Synergy in Materials: Leveraging Phosphosilicate Waste Forms for Electrochemical Salt Waste***," by Evarts et al. [19]. This was a study evaluating the addition of sodium borosilicate (NBS) glass additions of 2.5–30 mass% NBS-3 to the DPF5-336 reference material composition (after dechlorinating ERV3 salt simulant) based on recommendations by Ebert and Fortner [27]. The study found that the chemical durability was improved compared to the sample without added NBS-3 glass (0%) with a maximum durability improvement realized at 5 mass% NBS-3. Improvements over the DPF5-336 reference material were also seen at 10% NBS-3, but lower durabilities were observed at NBS-3 loadings of >10 mass%. The distribution of Cs was found homogeneously within the phosphate glass matrix phase, but it was associated with Fe and P in the crystalline portions of these samples.

#24 (2025) "***Phosphate-Based Approaches for Dechlorination and Treatment of Salt Waste from Electrochemical Processing of Used Nuclear Fuel: A Perspective on Recent Work***," by Evarts et al. [51]. This paper consolidates and summarizes methods for dehalogenating salt waste, which are applicable to pyroprocessing methods used for reprocessing used nuclear fuel (UNF) as well as potential use cases for salt-recycling for molten salt reactor (MSR) concepts. Highlights are provided in this paper of work that was done in a short timeframe around the publication of this work regarding phosphate waste form formulation, fabrication, and testing.

#25 (2025) "***Evaluation of Processing Conditions for the Reduction of Electrochemical Salt Waste Using Phosphate-Based Dechlorination***," by Werth et al. [52]. This paper summarizes experiments performed to evaluate processing temperature, environment (i.e., argon or air), and the ratio of H_3PO_4 to salt waste chloride (Cl^-:H^+) on the efficiency of dechlorination. The salt simulants used in this study were a simple alkali salt mixture (SSM) and ERV3. A comparison is provided in this document that summarizes the advantages and disadvantages of utilizing ADP or H_3PO_4 for dechlorination, which are summarized in Table A-1 (Appendix A).

#26 (2025) "***Evaluating High-Halide Waste Form Options for Salt-Based Nuclear Waste Simulants***," by Bai et al. [53]. This report summarizes a range of different glass systems that were evaluated for direct incorporation of ERV3 salt simulant, which included a pre-vitrified

$40Fe_2O_3$-$60P_2O_5$ binary glass frit. Results from the slow-cooling heat-treatment showed crystallization of alkali-iron-phosphate phases and higher loading amounts of ERV3 facilitated greater extent of crystal formation. The mass loss during/after heat-treatment is most likely the result of the volatilized ERV3 salt components.

#27 (2025) "***Technoeconomic Analysis for Evaluating Nuclear Salt Waste Form Technologies***," by Riley and Vienna [54]. This report (done under ARPA-E ONWARDS Project "HAWAII") summarizes work done to evaluate a scale-up process with associated costs to do large-scale dehalogenation of salt wastes using phosphate precursors and subsequently vitrify. The results from this study were compared to costs associated with the GBS-CWF process. The main takeaway is that the cost of the phosphate process could be significantly lower than the GBS-CWF process (i.e., 50% lower) due to the simplified process and the drastic increase in overall salt cation loading.

#28 (2025) "***Developments in Processing Criteria for Iron Phosphate Waste Form Design for Treating Electrorefiner Salt Wastes***," by Werth et al. [55]. This report summarizes some of the work done under the DE-NE0009317 NEUP project, including dechlorination experiments with the autotitrator, corrosion tests performed on different candidate crucible materials (i.e., Inconel 693, Stainless Steel 316L, Monofrax K3 refractory, alumina, and fused quartz) in iron phosphate melts with a summary provided of the results in Table A-2 (Appendix A), and waste form synthesis data collected on a range of iron phosphate glasses with different Fe/P molar ratios (0.1303–1.5635) and O/P molar ratios (3.3376–5.4304). Additional data on the waste forms is provided elsewhere [56].

#29 (2025) "***Final Report: Investigation into the processing parameters of phosphate-based dehalogenation for chloride-based waste salt***," by Carlson et al. [57]. This report is the final UNR-led report summarizing all the work that was done under the DE-NE0009317 NEUP project, including corrosion tests on containment materials, dechlorination tests, and waste form studies.

#30 (2025) "***Synthesis and Crystal Structures of Alkali (Na, Rb, Cs) Iron Phosphate Crystals***," by Chong et al. [58]. This report (done under ARPA-E ONWARDS Project "HAWAII") covers the synthesis process used to produce single crystals of $NaFeP_2O_7$, $RbFeP_2O_7$, and $CsFeP_2O_7$ and how they were characterized with single crystal XRD, SEM-EDS, and OM. All three of these crystals fall into the monoclinic $P2_1/c$ space group with similar unit cell parameters. The reason that these crystals were produced in the first place was to understand the properties of these types of crystalline phases (e.g., chemical durability that was not yet run) that have been observed to form in several of the iron phosphate waste form samples produced within the other studies discussed within this report.

#31 (2026) "***Corrosion Durability of Phosphate-Based Waste Forms***," by Liao et al. [59]. This report summarizes the chemical durability (ASTM C1308) testing results for phosphosilicate glasses produced with Fe_2O_3 and 5 mass% NBS-4, NBS-6, or Corning C7056 silicate glass. Additionally, three glasses were made without Fe_2O_3 but with 15 mass% NBS-3, NBS-4, or NBS-6 silicate glass. Pictures of all samples tested are provided in Figure A-13 (Appendix A). More details are provided elsewhere on these samples [20].

#32 (2026) "***Glass-Bonded Monazite Waste Forms for Lanthanide and Actinide Immobilization: From Theoretical Design to Scale-Up Production and Characterization***," by Peterson et al. [60]. This paper (done under ARPA-E ONWARDS Project "HAWAII") summarizes a scaled (1.6-kg) production of iron-phosphate-bonded monazite ($NdPO_4$). The key takeaway from this work is that this process can be scaled and the chemical durability of the overall product was very good ($NL_P \approx 10^{-4}$ g/m^2 over >200 days in ASTM C1220 coupon tests). An overview of the results found for this sample are shown in Figure A-14 (Appendix A).

#33 (2026) "***Evaluation of Iron-Phosphate Glass–Ceramic Waste Form for Electrorefiner Salt Waste Simulant Dechlorinated with Phosphoric Acid***," by Werth et al. [56]. This paper summarizes iron phosphate glass ceramic production based on a dechlorinated simplified electrorefiner salt simulant (48LiCl-33KCl-19NaCl mol). In this study, a matrix of glasses was produced that ranged with different Fe/P molar ratios (0.1303–1.5635) and O/P molar ratios (3.3376–5.4304). A diagram of the ternary for this work is found in Figure A-15 (Appendix A).

#34 (2026) "***Silicate-Modified Phosphate Waste Forms: Phase Partitioning and Durability for Salt Waste***," by Evarts et al. [20]. This paper summarizes an extended study from the related 2025 study [19] where 5 mass% of three additional silicate glasses (i.e., NBS-4, NBS-6, and Corning Glass C7056) were added to the DPF5-336 composition (after dechlorinating ERV3 salt simulant) to assess whether this resulted in any chemical durability improvements. The major finding is that the 5 mass% NBS-3 sample was better than the three new samples. Additionally, this work included three samples produced without Fe_2O_3 and the chemical durabilities of these samples were 3 orders of magnitude poorer than the equivalent samples made with Fe_2O_3.

#35 (2026) "***Process Effects and Structural Analysis on Phosphate Intermediates during Dechlorination of Mixed Chloride Waste Product for Nuclear Waste Immobilization***," by Greiner et al. [61]. This paper summarizes structural evaluation for iron phosphate glasses produced from dechlorinating SSM or ERV3 simulants with H_3PO_4 at P:Cl = 1:1 (molar) under air or argon atmospheres. Structural evaluations were performed using high-performance liquid chromatography (HPLC) and Raman spectroscopy.

#36 (2026) "***Structural, Chemical, and Thermal Characterization of Novel Tin Fluorophosphate Nuclear Salt Waste Forms***," by McGuire et al. [62]. This paper summarizes glass formation and measured properties for a series of glasses produced in the $x SnF_2 \cdot 10SnO \cdot (90\text{-}x)P_2O_5$ system. The measured chemical durabilities (ASTM C1308) of these glasses were lower than desired.

2.1.2 Summary of Relevant and Related Studies Outside Phosphates

In addition to this work, parallel/related efforts are summarized below, which include other types of dehalogenation investigations. The reason that these are documented within this report as they justify why the phosphate waste form processes are not going forward for more research for the time being – the reason being that other options show a much higher potential for improved waste loadings (e.g., organic acid dehalogenation; see Figure 4-1).

Investigation of other dehalogenation reagents, i.e., organic acids:

- **(2025)** "***Organic Acid-Assisted Thermal Dehalogenation of Halide Salt Nuclear Wastes: From Waste Salts to Borosilicate Glass***," by Oshiro et al. [22]. This paper summarizes work that was done to evaluate five separate organic acids to dehalogenation chloride salts including oxalic, formic, acetic, oxamic, and citric where oxalic proved the most effective. A glass, called TARS, was produced assuming that full dechlorination could be achieved for ERV3 salt and several properties were measured, including melt viscosity (η), product consistency testing (PCT), ASTM C1220 testing (MCC-1), density, glass transition temperature (T_g), and liquidus temperature (T_L). The measured values fell within model-predicted values using composition-property models from Hanford Waste Treatment and Immobilization Plant (WTP) low-activity waste (LAW).

- **(2026)** "***Organic Acid Dehalogenation and Borosilicate Glass Waste Form Testing (TARSv2)***," by Oshiro et al. [63]. This report summarizes dechlorination experiments

performed with oxalic acid and different salt compositions along with a series of eight glasses (i.e., TARSv2-ID1 – TARSv2-ID8). Dechlorination using oxalic acid proved challenging for KCl but worked very well for LiCl. Of the eight glasses tested, three showed high promise in most of the characterization categories (i.e., crystallography, viscosity, electrical conductivity, liquidus temperature, etc.), including TARSv2-ID1, TARSv2-ID4, and TARSv2-ID5. Chemical durability data for these glasses are provided in [64].

- **(2026)** "***Corrosion Tests with Developmental TARS Materials***," by Schneiderlochner et al. [64]. This report summarizes corrosion tests (ASTM C1220, ASTM C1285, and ASTM C1308) that were run with the glasses (TARSv2-ID1 – TARSv2-ID8) produced assuming organic-acid dechlorination of ERV3 from the study by Oshiro et al. [63]. The general ranking of these materials in order from best performer to worst performer was the following: ID1 > ID5 > ID4 > ID2 > ID3 > ID8 > ID6 > ID7. TARSv2-ID1 was recommended for further testing.

Fluoride-salt work – defluorination:

- **(2022)** ***Thermal Conversion in Air of Rare-Earth Fluorides to Rare-Earth Oxyfluorides and Rare-Earth Oxides***," by Chong and Riley [65]. In this paper, thermal defluorination was evaluated for rare-earth fluoride (REF_3) compounds (RE = La, Ce, Pr, Nd, Tm, Yb, and Lu) at temperatures of 400–1400°C. All compounds showed conversion to REO_x (mixed oxides) and/or REOF (oxyfluoride) compounds.

Foundational study published just before the Road Map Report that is summarized here:

- **(2020)** "***Corrosion Behavior of Developmental Iron Phosphate Glass Waste Forms: FY20 Status Report***," by Stariha et al. [35]. This report documents the chemical durability data for the 2020 study by Riley et al. that set the foundation for the remaining work done in this area. The results showed that durability of glasses made with < 27 mol% Fe_2O_3 were poor and additions of ≤ 34 mol% Fe_2O_3 did not improve durability. The compositional window of study was bound by four compositions, i.e., DPF3-67, DPF3-89, DPF5-309, and DPF5-336 shown in the ternary diagram in Figure A-1 (Appendix A).

2.2 Summary of Salt Simulants Evaluated

The work that has been done to evaluate phosphate-based reagents has utilized a range of different salt compositions, which are summarized below in Table 2-1. These include SSM [52, 61], ER(SF) [14], ERV [62], ERV2 [14, 66], ERV3 [19, 20, 34, 36, 52, 53], KCl [15], CsCl [15], and ORH [62]. In all cases, these types of salts were assessed as simulants to represent more complex salts expected in the electrorefiner (ER) after fuel batch processing except for ORH, which is after oxide reduction (OR). Simpler, single-component salts were used in some cases to allow for less heterogeneity within the multi-salt batches [e.g., ER(SF), ERV2, ERV3].

Table 2-1. Summary of salt simulant compositions (mass%) utilized in phosphate-based work in recent years. See the text above for example studies in which these salts were used.

Salt	CsCl	ER(SF)	ERV	ERV2	ERV3	KCl	ORH	SSM
$CeCl_3$	–	0.002	1.8	5.00	5.00	–	–	–
CsCl	100.00	5.18	2.3	–	7.01	–	–	–
CsI	–	–	–	7.00	–	–	–	–
KCl	–	40.52	43.1	38.68	39.06	100.00	–	44.29
KI	–	3.09	–	–	–	–	–	–
$LaCl_3$	–	1.55	–	–	–	–	–	–
Li_2O	–	–	–			–	10	
LiCl	–	33.09	33.9	32.32	32.05	–	70	36.29
NaCl	–	9.88	11.3	9.00	9.01	–	–	19.42
$NdCl_3$	–	2.01	5.1	5.00	4.87	–	–	–
$SrCl_2$	–	3.13	2.5	3.00	3	–	20	–
YCl_3	–	1.55	–	–	–	–	–	–

2.3 Summary of the Glass Binders Evaluated

Four different silicate glass binders were utilized for the studies documented within this report. The compositions of these four glasses are listed below in Table 2-2. Of these four glasses, three are developmental compositions that come from a 2017 study by Riley et al. [5] to assess high-silicate binders for the GBS-CWF process, and one is a commercial glass from Corning called C-7056 (noted as alkali borosilicate in the technical data sheet).

Table 2-2. Summary of silicate glass binder compositions (mass%), including composition (if known), processing temperature used to vitrify the glass, the bulk density (ρ_b), glass transition temperature (T_g), softening point (T_s), the coefficient of thermal expansion (CTE) at two different temperature ranges, and references for studies where these glasses were utilized. Standard deviations are provided for some of the values where available. These values come from Riley et al. [5] and from the 7056 Technical Data Sheet from Corning [67].

Property	Glass ID			
	NBS-3	NBS-4	NBS-6	C-7056
SiO_2	58.88	58.87	49.02	proprietary
B_2O_3	8.98	8.98	18.80	
Al_2O_3	8.98	5.99	8.65	
CaO	–	3.99	–	
Na_2O	20.17	20.17	20.17	
ZrO_2	2.99	2.00	3.36	
T_p (°C)	1550	1550	1350	–
ρ_b (g/cm^3)	2.4851 (±0.0015)	2.5247 (±0.0017)	2.5290 (±0.0004)	2.29
T_g (°C)	553.9 (±0.1)	543.0 (±0.3)	544.9 (±1.3)	512
T_s (°C)	593.8 (±5.5)	582.8 (±0.4)	581.5 (±2.2)	718
CTE (×10^{-6} K^{-1}; $T < T_g$)	10.24 (±0.09)	10.99 (±0.32)	10.64 (±0.04)	5.15
CTE[(a)] (×10^{-6} K^{-1}; $T_g < T < T_s$)	75.20 (±2.55)	72.43 (±3.79)	86.25 (±1.57)	–
Reference(s)	[19, 20]	[20]	[20]	[20]

3.0 Updates to the Road Map

In 2021, a joint PNNL-ANL report was published titled "*Road Map for Developing Iron Phosphate Waste Forms for Salt Wastes*" [1] that summarized the key issues with phosphate-based processing of waste salts, the current state of research, and the proposed gaps and approaches to fill the gaps, which are all summarized in *Appendix B – Road Map Categories*. The primary categories identified included: *Waste Composition* (see Table 3-1 and Table B-1, Appendix B), *Matrix and Additives* (see Table 3-2 and Table B-2, Appendix B), *Waste Processing* (see Table 3-3 and Table B-3, Appendix B), *Waste Form Properties* (see Table 3-4 and Table B-4, Appendix B), *Waste Form Acceptance* (see Table 3-5 and Table B-5, Appendix B), and *Waste Form Performance* (see Table 3-6 and Table B-6, Appendix B) [1], where updates to the Road Map are summarized in the tables below.

Table 3-1. Summary of **Waste Composition** issues identified, approaches to fill gaps, and updates since the Road Map [1] was written in 2021. See Table B-1 (Appendix B) for the original list.

Issues Identified	Approaches to Fill Gaps	Updates Since Road Map
The range of ER and OR salt waste compositions that will ultimately be produced has not been clearly defined. The waste composition and characteristic ranges are needed to support waste form, process design, and disposal qualification activities.	Electrochemical process development, waste form design, waste processing, and disposal requirements need to be developed concurrently due to the potential feedback effects of each technology component on the others. By doing so, the ranges of key waste component concentrations and waste characteristics will be refined.	Several ER-related and some OR-related studies were performed, including glass-formation, waste form testing, and other characterizations; this covers all the studies documented in Section 2.1.1. see descriptions in Section 2.2 and Table 2-1.
Several chloride and fluoride salt mixtures are being considered by MSR designers. For MSRs, salt compositions vary depending on vendor design and operating strategy. The range of halide salt wastes generated from prototypical MSRs are needed.	Work with other organizations within DOE-NE and the potential MSR vendors to develop a database of fuel compositions and characteristics. Select an example salt composition from the list for use in waste form and process development activities.	*This was not done*. However, some of this will be done for molten chloride fast reactor (MCFR) salt wastes in a new project that started in August 2026 funded out of University of Utah (*Principal Investigator: Professor Michael Simpson*) [68] where phosphate-based reagents and organic acids will be evaluated for dechlorination.

Table 3-2. Summary of **Matrix and Additives** issues identified, approaches to fill gaps, and updates since the Road Map [1] was written in 2021. See Table B-2 (Appendix B) for the original list.

Issues Identified	Approaches to Fill Gaps	Updates Since Road Map
Alkali-phosphate and alkaline earth-phosphate glasses, *without glass-forming additives*, are not sufficiently durable to serve as a waste form. Additives such as Fe_2O_3 and Al_2O_3 can be used to improve chemical durability but require higher-temperature vitrification in a separate processing step. Some composition regions are prone to crystallization and form phases that may be detrimental to processing or performance. Adequate compositions are required for phosphate glasses that are processable and durable with dehalogenated salt wastes as major components of the glasses.	Design and test phosphate-based glasses with a range of different salt compositions, additives, and waste loadings to survey the boundaries of acceptable glass formation.	Several studies were performed that utilized different glass-formers (e.g., Al_2O_3 in place of Fe_2O_3) [40] and other additives (e.g., SnF_2, SnO) [62]. While exchanging some Fe_2O_3 with Al_2O_3 showed improvements in chemical durability, SnF_2 and SnO did not improve overall durability.
Nuclear waste glass design, qualification, and process control all rely heavily on the ability to predict glass properties as functions of key composition and processing related parameters. Few if any such models are available for iron-phosphate based glasses.	Develop glass property-composition data and associated models over the range of likely glass compositions. These data and models should include properties such as durability response, processability related properties, and glass forming ability.	This was attempted for aluminophosphate glasses based on the literature available, but the chemical durability data available in the literature was collected under too large of a variety of testing conditions [40, 48]. The takeaway from that study was that adding Al_2O_3 and/or Fe_2O_3 to high-alkali phosphate glasses significantly improves chemical durability. Both Fe and Al cations cross-linked phosphate chains, forming P−O−Fe and P−O−Al bonds, which help stabilize the glass structure.

Table 3-3. Summary of **Waste Processing** issues identified, approaches to fill gaps, and updates since the Road Map [1] was written in 2021. See Table B-3 (Appendix B) for the original list.

Issues Identified	Approaches to Fill Gaps	Updates Since Road Map
A single-step process is preferred for simplicity and scale-up, but the system does not operate as desired during single-step scoping tests.	Evaluate alternative options for making the 1-step process work effectively.	*This was not done.* Several challenges were noted in the first study where this was attempted [14]. However, a new system design was created to attempt these experiments but was not built/tested [41].
Reactant optimization for different chloride salt wastes (e.g., H_3PO_4 vs ADP; different Fe additives).	Evaluate different phosphate precursors for different chloride salt streams.	Three phosphate reagents were evaluated, including ADP [14, 15, 20, 51], DHP [14], and H_3PO_4 [16, 52] across several studies. A different Fe additive ($FePO_4$) was assessed on a separate project [60].
Dehalogenation and immobilization reactions require evaluation of fluoride salts.	Perform initial dehalogenation tests with H_3PO_4 and ADP. Evaluate other potential reactions.	This was not done. Defluorination would require a complete redesign of the off-gas system to manage HF(g).
Integrated process tests are needed to determine adequacy of materials flows and determine partitioning between process streams.	Perform laboratory/bench-scale integrated process tests, develop reaction rates and process flow sheets. Separate tests may need to be done for waste forms made with different salt types.	*This was not done.*
Evaluate off-gas stream compositions, treatment requirements, and treatment methods.	Evaluate off-gas generation, neutralization, and need for recycling and treatment. Develop and test off-gas treatment/recycle methods.	Autotitration was performed at UNR to track HCl production through neutralization with NaOH titrant [55, 57].
Process ranges are not determined.	Perform integrated process tests over range of key processing parameters. Determine processing success boundaries and develop process models (may need to be done for different salt types).	Several parameters were evaluated in experiments studying dechlorination atmosphere (air, Ar), temperature, and reagent (i.e., ADP, H_3PO_4) [52, 55, 57].
Process equipment remote operation and maintenance.	Evaluate methods to remotize process equipment and demonstrate effective hands-off operations and control.	A conceptual design was created and published for a fully operational device (DeVA) that could be fabricated to run in a hot cell [41].
Scale-up testing is required to evaluate overall system performance (e.g., process rates, component partition factors)	Scale-up integrated process tests from laboratory-scale to pilot scale (may need to be done for different salt types).	Total glass batches were scaled up from 10-20 g [14] to ≈ 30 g [30] and then ≈ 66 g [15].
Determine process equipment lifetime and replacement requirements.	Study materials corrosion processes at laboratory scale. Design equipment and test equipment lifetime thought scaled testing of individual components and integrated systems.	Some corrosion tests were performed on a range of materials for dechlorination studies (i.e., alumina, silica, glassy carbon, boron nitride, Ni) [14] as well as for vitrification of iron phosphate melts (i.e., Inconel 693, stainless steel 316L, and Monofrax K3) [55] [57].
Determine safety concerns from processes required to make iron phosphate waste forms.	Determine how/if these hazards can be effectively mitigated.	This was not (*officially*) done but some thought was given to how to handle H_3PO_4, H_2O, HCl, and NH_4Cl within the hot during the design of the DeVA [41].
Safeguards and materials accountancy.	Evaluate safeguards and materials accountancy under regulations established by the NRC.	*This was not done.*

Table 3-4. Summary of **Waste Form Properties** issues identified, approaches to fill gaps, and updates since the Road Map [1] was written in 2021. See Table B-4 (Appendix B) for the original list.

Issues Identified	Approaches to Fill Gaps	Updates Since Road Map
Waste glasses tend to crystallize during slow cooling after melting.	More data are needed to evaluate properties of CCC-treated WFs including what crystals form and how they affect glass properties of interest.	Several slow-cooling studies were performed on iron phosphate glasses [19, 20, 30, 34, 36, 40] and aluminophosphate glasses [40]. From these studies, the microstructures and phase distributions are very complicated. Several crystalline phases [e.g., $K_{7.33}Fe_{10}(PO_4)_{12}O_{0.66}$, $Li_3Fe_2(PO_4)_3$, $LiFePO_4$, $CsFeP_2O_7$, $SrFe(P_2O_7)_2$, Sr_2CeO_4, $K_{10}Sr_7(P_2O_7)_5O_2$, $SrCeO_3$, and $KSrPO_4$, $FePO_4$, $REPO_4$ (monazite, xenotime)] were documented to form upon slow cooling that can have negative impacts on residual glass chemical durability.
Crystallization can occur during CCC, which can lead to cracking and embrittlement of the WF.	Evaluate the chemical and physical robustness of CCC-treated phosphate glasses.	Cracking and embrittlement were observed after CCC treatments in all samples investigated [19, 20, 30, 34, 36, 40]. This was attributed to the mismatch in coefficients of thermal expansion (CTE) within the glass phase(s) and crystalline phases present in these samples. It is possible that these issues could be minimized if cooling through critical temperature ranges (i.e., softening point, T_s, and glass transition temperature, T_g) were slowed down even further through a more controlled cooling.
Few studies exist in the literature on the thermal stability of phosphate glasses (including compositions expected from these salt streams).	Evaluate thermal stability of these glasses.	Limited thermal analysis (i.e., thermogravimetric analysis or TGA) was done on iron phosphate melts to assess thermal stability [16].
Few studies exist in the literature on the radiological stability of phosphate glasses (including compositions expected from these salt streams).	Evaluate radiological stability of these glasses.	*This was not done*.
Determine if waste form should remain in crucible and be placed into a canister or be poured into a canister. Determine if radiation dose and heat from waste form with high waste loading require a special storage facility or longer cooling times before transport and disposal.	Determine thermal properties and thermal limits of iron phosphate waste forms.	Some work was done to consider options for in-container vitrification during the technoeconomic assessment (TEA) [54].

Table 3-5. Summary of **Waste Form Acceptance** issues identified, approaches to fill gaps, and updates since the Road Map [1] was written in 2021. See Table B-5 (Appendix B) for the original list.

Issue Identified	Approaches to Fill Gaps	Updates Since Road Map
The chemical durabilities of phosphate glasses vary significantly with minor differences in composition.	Evaluate consistency and regulatory acceptability for phosphate glasses made with different salt waste streams.	A wide range of chemical durability testing was conducted on phosphate glasses with more details provided in Section 2.1.1 [29, 31, 32, 39, 42, 59, 64]. These cover a variety of different compositional sets from fixed waste loading at different Fe:P ratios (DPF3 series) [35], different waste loadings with fixed Fe:P ratios (DPF5 series) [35, 39], the same compositions but with added silicate glass (NBS-3) at different amounts [50], the same composition with 5 mass% of silicate glasses (i.e., NBS-3, NBS-4, NBS-6, Corning C7056) added to assess impacts on chemical durabilities [59].

Table 3-6. Summary of **Waste Form Performance** issues identified, approaches to fill gaps, and updates since the Road Map [1] was written in 2021. See Table B-6 (Appendix B) for the original list.

Issue Identified	Approaches to Fill Gaps	Updates Since Road Map
Understanding composition effects on quenched glass chemical durability are limited. Need to determine the mode of radionuclide release and WF degradation. Determine if WF acceptance criteria developed for BS glass WFs are appropriate for iron phosphate WFs. Determine the effect of dissolved phosphate species on solubility limits and transport behaviors of radionuclides used to assess repository performance.	More work is needed to evaluate the chemical durability of quenched and CCC-treated glasses of varying WLs and compositions. Also, the effects of phosphate on seepage water and chemistry of radionuclides should be studied.	Several studies were published document and discuss chemical durability results on a variety of phosphate compositions [32, 39, 42], including that of CCC-cooled glasses [29, 31, 35, 39, 50, 59].

4.0 Comparisons between Options

The salt cation loading limits for phosphate-based products are limited to around 15–16 mass% before the chemical durability suffers. A summary of these iron phosphate data points (i.e., P1, P2, P3, DPF5-336) are shown in blue within Figure 4-1 below. In this figure, the salt cation loading (WL_{sc}) and waste form volume to immobilize a given mass of starting salt ($V_{wf,s}$) are compared for a variety of different waste form types. More details about these comparisons are provided elsewhere [22, 63, 69], but data was generated using Equation (8) and Equation (9) where $f_{sc,wf}$ denotes the fraction of salt cations in the waste form, ρ_{wf} is the bulk density of the waste form, ϕ is the porosity (vol%), $f_{sc,s}$ is the mass fraction of salt cations in the salt being immobilized or dehalogenated, and $f_{wl,wf}$ is the waste loading in the waste form. The reason for comparing the salt cation loading (WL_{sc}) and not the full salt loading (m_s) is that several different technologies demonstrated in the literature include a dehalogenation step prior to waste form fabrication, thus comparing them on a full-salt basis rather than salt-cations-only basis is misleading.

$$V_{wf,s} = \left[\frac{WL_{sc}}{(f_{sc,wf})(\rho_{wf})\left(1 - {}^{\phi}/_{100}\right)}\right] \tag{8}$$

$$f_{sc,wf} = (f_{sc,s})(f_{wl,wf}) \tag{9}$$

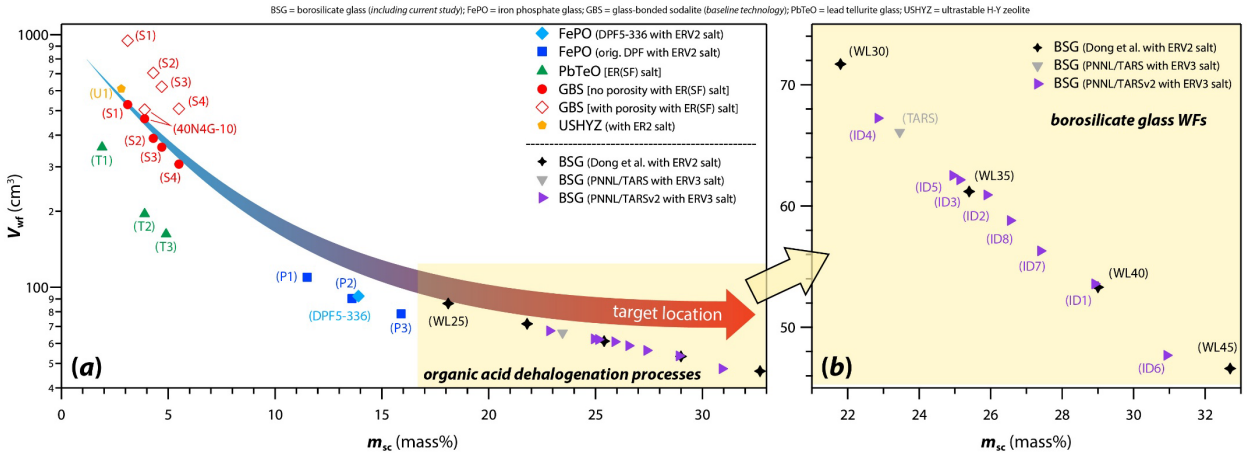

Figure 4-1. Summary of the calculated waste form volume (starting from 100 g salt) versus salt cation mass loading in various waste forms, including (a) several waste forms and (b) a magnified view of the organic acid dehalogenation samples resulting in borosilicate glass (BSG) waste forms; the phosphate waste forms are denoted in blue as P1, P2, P3, and DPF5-336. This figure was modified from previous versions by Riley [69] and Oshiro et al. [22] to include the new TARSv2 compositions. Note that part (a) is a semi-log plot. See text for descriptions of the other waste forms. This figure comes from Oshiro et al. [63].

5.0 Summary and Conclusions

Several studies have been performed on related topics around phosphate-based dechlorination of electrorefiner salt waste streams as well as evaluating vitrification of the resulting products from these processes into high-durability waste forms. Of the work done to date, here are some of the most notable conclusions:

Related to Dehalogenation Processes:

- Dehalogenation processes evaluated based on H_3PO_4 as a reagent require calcination of the acid to a solid product, which will drive off a lot of water that has to be managed. Also, H_3PO_4 is a strong acid so that adds additional hazards where the major byproducts are water and HCl(*g*,*l*).

- Dehalogenation processes evaluated based on ADP and DHP vary in efficiency. The ADP-based dehalogenation works well but requires higher temperatures than H_3PO_4 (≈ 600°C vs < 400°C). Also, DHP did not work as well as expected compared to ADP in a head-to-head experiment, despite having double the ratio of NH_4^+:Cl^- [14]. Both processes result in the production of water and NH_4Cl byproducts that can be captured in a liquid scrubber or condenser.

- Using phosphate-based reagents for dehalogenation has some limitations. First, using nitrogen-based reagents (e.g., ADP, DHP) with some halide compounds can result in the production of *highly hazardous byproducts*, some of which are known *contact explosives* (i.e., NI_3, NH_4I_3). Second, using phosphate-based precursors results in residual phosphate byproducts left over after the reaction. Because of this, the overall waste loading in the waste form will always be diluted by this phosphate contribution and the amount of phosphate reagent used has to be optimized for each salt mixture to (a) maximize salt cation in the final product, (b) minimize phosphate diluent, and (c) maximize dechlorination efficiency. Thus, while excess phosphate reagent can be added to help drive the dechlorination reactions to completion (i.e., $NH_4^+ >> Cl^-$, $H^+ >> Cl^-$), this just dilutes the waste (salt cation) loading in the final product after vitrification.

Related to Waste Form Processes:

- The most promising compositions are in the Fe_2O_3-P_2O_5 glass system, and this is around the $40Fe_2O_3$-$60P_2O_5$ composition.

- Slow cooling (e.g., canister centerline cooled) waste forms tend to heavily crystallize. This crystallization leads to the glass-phase constituents being pulled out of the melt and this can leave the residual melt in a state that is much less optimal in terms of chemical durability.

- The most durable crystalline phases observed in slow-cooled waste forms are of the $REPO_4$ (monazite, xenotime) family. These crystals form in the melt and tend to precipitate out and settle towards the bottom of the sample. In some cases, however, $REPO_4$ crystals have been seen throughout the sample.

- For high-Li salt streams (e.g., LiCl-KCl eutectic from electrochemical processing), the most prominent crystalline material found in slow-cooled waste forms are alkali iron phosphate phases [i.e., $Li_3Fe_2(PO4)_3$] [20].

- Adding silicate glass at a loading of ≈ 5 mass% to the dechlorinated product and Fe_2O_3 and vitrifying can improve the overall leach rate of the waste form.

- While replacing some Fe_2O_3 with Al_2O_3 shows improvements in chemical durability (Figure A-8 and Figure A-12, Appendix A), replacing all Fe_2O_3 with Al_2O_3 showed a notable decrease in chemical durability. Additional work could be done to assess the optimal ratio of P_2O_5, Al_2O_3, and Fe_2O_3 to maximize chemical durability in waste forms of similar (or a target) waste loadings.

- Other glass formers and intermediates (than Fe_2O_3 with Al_2O_3) can be assessed to further improve chemical durability.

Lastly, the salt cation loading potential in phosphate waste forms is limited by several factors. First, the dehalogenation potential and efficiency are driven by the molar ratio of the phosphate reagent cations (i.e., NH_4^+, H^+) to the halide fraction (i.e., Cl^- + I^-), but adding excess phosphate reagent results in diluted salt cation loading in the dehalogenated product. Second, the phosphate work is ending for now because a replacement option was identified that includes using organic acids to dehalogenate the salt whereby the dehalogenated products can be directly vitrified and the reagent anions are decomposed to oxides (i.e., oxalates → carbonates → oxides). The organic-acid approach for dehalogenation has potential to drastically improve salt cation loadings by > 2× over the phosphate-based approaches summarized within this report – see Figure 4-1.

6.0 Recommendations for Future Work

Lastly, some actions highlighted as not being completed within Section 3.0 based on recommendations made in the Road Map Report [1] are listed below and could use further attention in follow-up studies:

- **Work with other organizations within DOE-NE and the potential MSR vendors to develop a database of fuel compositions and characteristics and then select an example salt composition from the list for use in waste form and process development activities.** While this was not directly done within the timeframe covered within this report (i.e., 2021–2026), some of this will be done for molten chloride fast reactor (MCFR) salt wastes under a new IRP Project that started in August 2026 (Principal Investigator: Professor Michael Simpson, University of Utah) [68].

- **Perform laboratory/bench-scale integrated process tests, develop reaction rates and process flow sheets.** This could be done but will likely be done with other dechlorination reagents instead of phosphates.

- **Evaluate safeguards and materials accountancy under regulations established by the NRC.** This is a process that could be conducted down the road once more mature compositions and flowsheets are established. However, this is unlikely to occur for iron phosphate formulations.

- **Evaluate radiological stability of phosphate glasses that are relevant to the compositions of importance for this application, e.g., dehalogenated high-LiCl/KCl salts.** While this was not done, some radiation stability evaluations have been conducted for phosphate glass materials and are summarized in one of the documents covered in Section 2.1.1.

- **Evaluate chemical durabilities and other properties of commonly found and commonly reported crystalline phases present in these types of waste forms upon CCC cooling.** These crystals include phases like $Li_3Fe_2(PO_4)_3$, $NaFeP_2O_7$, $KFeP_2O_7$, $CsFeP_2O_7$, and monazite/xenotime ($REPO_4$) crystals. Very little information is available on these types of compounds within the scientific literature.

7.0 References

[1] Riley, BJ, JD Vienna, and WL Ebert. 2021. *Road Map for Developing Iron Phosphate Waste Forms for Salt Wastes*. PNNL-30998, ANL/CFCT-20/44, Pacific Northwest National Laboratory, Richland, WA.

[2] Ebert, WL. 2005. *Testing to Evaluate the Suitability of Waste Forms Developed for Electrometallurgically-Treated Spend Sodium-Bonded Nuclear Fuel for Disposal in the Yucca Mountain Repository*. ANL-05/43, Argonne National Laboratory-East, Argonne, IL.

[3] Priebe, S and K Bateman. 2006. "The ceramic waste form process at the Idaho National Laboratory." *Nuclear Technology* **162**(2):199–207.

[4] Bateman, KJ, CJ Knight, and CW Solbrig. 2007. *Current Status of Ceramic Waste Form Development*. INL/INT-06-11736, Rev. 1, Idaho National Laboratory, Idaho Falls, ID.

[5] Riley, BJ, JD Vienna, SM Frank, JO Kroll, JA Peterson, NL Canfield, Z Zhu, J Zhang, K Kruska, and DK Schreiber. 2017. "Glass binder development for a glass-bonded sodalite ceramic waste form." *Journal of Nuclear Materials* **489**:42–63.

[6] Gesualdi, JE, E Schneiderlochner, Y Liao, J Rojas, and WL Ebert. 2026. *Direct Processing of Lithium Chloride Based Waste Salt in a Ceramic Waste Form*. ANL/CFCT-26/3, Argonne National Laboratory, Lemont, IL.

[7] Yoo, T-S, A Moudgal, and W Yang. 2026. *Progress Report for Brine-Loading Process Feasibility Validation*. INL/RPT-26-95056, Idaho National Laboratory, Idaho Falls, ID.

[8] Riley, BJ, BT Rieck, JS McCloy, JV Crum, SK Sundaram, and JD Vienna. 2012. "Tellurite glass as a waste form for mixed alkali-chloride waste streams: candidate materials selection and initial testing." *Journal of Nuclear Materials* **424**(1-3):29–37.

[9] McCloy, JS, BJ Riley, AS Lipton, CF Windisch, NM Washton, MJ Olszta, and CP Rodriguez. 2013. "Structure and Chemistry in Halide Lead–Tellurite Glasses." *The Journal of Physical Chemistry C* **117**(7):3456–3466.

[10] Riley, BJ, JO Kroll, JA Peterson, DA Pierce, WL Ebert, BD Williams, MMV Snyder, SM Frank, JL George, and K Kruska. 2017. "Assessment of lead tellurite glass for immobilizing electrochemical salt wastes from used nuclear fuel reprocessing." *Journal of Nuclear Materials* **495**:405–420.

[11] Riley, BJ, DA Pierce, JV Crum, BD Williams, MMV Snyder, and JA Peterson. 2018. "Waste form evaluation for $RECl_3$ and REO_x fission products separated from used electrochemical salt." *Progress in Nuclear Energy* **104**:102–108.

[12] Donze, S, L Montagne, and G Palavit. 2000. "Thermal conversion of heavy metal chlorides ($PbCl_2$, $CdCl_2$) and alkaline chlorides (NaCl, KCl) into phosphate glasses." *Chemistry of Materials* **12**(7):1921–1925.

[13] Siemer, DD. 2012. "Improving the integral fast reactor's proposed salt waste management system." *Nuclear Technology* **178**(3):341–352.

[14] Riley, BJ, JA Peterson, JD Vienna, WL Ebert, and SM Frank. 2020. "Dehalogenation of electrochemical processing salt simulants with ammonium phosphates and immobilization of salt cations in an iron phosphate glass waste form." *Journal of Nuclear Materials* **529**:151949.

[15] Riley, BJ, S Chong, and CE Lonergan. 2021. "Dechlorination Apparatus for Treating Chloride Salt Wastes: System Evaluation and Scale-Up." *ACS Omega* **6**(47):32239–32252.

[16] Murray, P, H Werth, S Sullivan, BJ Riley, M Simpson, C Lonergan, and K Carlson. 2024. "Phosphate-based dechlorination of electrorefiner salt waste using a phosphoric acid precursor." *ACS Omega* **9**(17):19395–19400.

[17] Chakrabarti, A, L Pereira, MI Ojovan, JS McCloy, S Schuller, H Hu, J Heo, W Um, W Deng, R Jia, and K Xu. 2026. "Nuclear waste immobilization: A review on phosphate glass-ceramics." *Journal of Nuclear Materials* **633**:157023.

[18] Xu, SG. 2026. "Decontamination of Chloride Salt Solvent from Spent Chloride Salt Fuel and Pyro–Electrometallurgical Processing Salt for Recycling—A Review." *Journal of Nuclear Engineering* **7**(2):38.

[19] Evarts, JS, BJ Riley, CE Lonergan, MS Harris, J Bai, E Bohannan, I Ajoku, S Chong, and JS McCloy. 2025. "Synergy in Materials: Leveraging Phosphosilicate Waste Forms for Electrochemical Salt Waste." *ACS Sustainable Resource Management* **2**(3):514–523.

[20] Evarts, JS, BJ Riley, HS Werth, Y Liao, Z Zhu, K Yano, and JA Silverstein. 2026. "Silicate-Modified Phosphate Waste Forms: Phase Partitioning and Durability for Salt Waste." *ACS Sustainable Resource Management (in press)*:DOI: 10.1021/acssusresmgt.1026c00382.

[21] Dong, Y, K Xu, Z Jia, C Niu, and D Xu. 2022. "Dechlorination and vitrification of electrochemical processing salt waste." *Journal of Nuclear Materials* **567**:153833.

[22] Oshiro, JM, H Hallikainen, BJ Riley, X Lu, B Iyer, B Merrill, V Goncharov, JM Westman, M Liezers, JL George, B Parruzot, JS Evarts, JD Vienna, JS McCloy, and X Guo. 2025. "Organic Acid-Assisted Thermal Dehalogenation of Halide Salt Nuclear Wastes: From Waste Salts to Borosilicate Glass." *Industrial & Engineering Chemistry Research* **64**(40):19484–19501.

[23] ASTM. 2021. *ASTM C1220-21, Standard Test Method for Static Leaching of Monolithic Waste Forms for Disposal of Radioactive Waste*. ASTM C1220-21, American Society for Testing and Materials International, ASTM International Book of Standards Volume 12.01, West Conshohocken, PA.

[24] ASTM. 2021. *ASTM C1285-21, Standard Test Methods for Determining Chemical Durability of Nuclear, Hazardous, and Mixed Waste Glasses and Multiphase Glass Ceramics: The Product Consistency Test (PCT)*. ASTM C1285-21, American Society for Testing and Materials International, ASTM International Book of Standards Volume 12.01, West Conshohocken, PA.

[25] ASTM. 2021. *ASTM C1308-21, Standard Test Method for Accelerated Leach Test for Measuring Contaminant Releases From Solidified Waste*. ASTM C1308-21, American Society for Testing and Materials International, ASTM International Book of Standards Volume 12.01, West Conshohocken, PA.

[26] ASTM. 2018. *ASTM C1663-18, Standard Test Method for Measuring Waste Glass or Glass Ceramic Durability by Vapor Hydration Test*. ASTM C1663-18, American Society for Testing and Materials International, ASTM International Book of Standards Volume 12.01, West Conshohocken, PA.

[27] Ebert, WL and JA Fortner. 2019. *Analyses of Iron Phosphate Glasses for Dehalogenated Salt Waste*. ANL/CFCT-19/5, Argonne National Laboratory, Lemont, IL.

[28] Chong, S, BJ Riley, and ZJ Nelson. 2021. "Crystalline compounds for remediation of rare-earth fission products: A review." *Journal of Rare Earths* **40**(3):365–380.

[29] Stariha, SA and WL Ebert. 2021. *Corrosion Behavior of Developmental Iron Phosphate Waste Forms: FY21 Status Report*. ANL/CFCT-21/14, Argonne National Laboratory, Lemont, IL.

[30] Riley, BJ and S Chong. 2021. "Effects of composition and canister centerline cooling on microstructure, phase distribution, and chemical durability of dehalogenated iron phosphate waste forms." *J. Non-Cryst. Solids* **579**:121319.

[31] Ebert, W. 2022. *Conceptual Iron Phosphate Waste Form Degradation Model*. ANL/CFCT-22/48, Argonne National Laboratory, Lemont, IL.

[32] Stariha, SA and WL Ebert. 2022. *Corrosion Behavior of Fast-Cooled Iron Phosphate Reference Material*. ANL/CFCT-22/49, Argonne National Laboratory, Lemont, IL.

[33] Riley, BJ and S Chong. 2022. "Dehalogenation reactions between halide salts and phosphate compounds." *Frontiers in Chemistry* **10**:976781.

[34] Riley, BJ, NL Canfield, M Peterson, JL George, S Chong, and JV Crum. 2023. *Crystalline versus Glassy Nature of Iron Phosphate Waste Forms Subjected to Different Slow Cooling Curves*. PNNL-34917, Pacific Northwest National Laboratory, Richland, WA.

[35] Stariha, SA and WL Ebert. 2020. *Corrosion Behavior of Developmental Iron Phosphate Glass Waste Forms: FY20 Status Report*. ANL/CFCT-20/34, Argonne National Laboratory, Lemont, IL.

[36] Riley, BJ, S Chong, and ET Nienhuis. 2023. *Canister Centerline Cooling Experiments for DPF5-336 Reference Material Made with ERV3b Salt Simulant*. PNNL-33802, Pacific Northwest National Laboratory, Richland, WA.

[37] Amoroso, J and M Kesterson. 2023. *Calculation of CCC Profiles for Nonstandard Canisters*. SRNL-L3310-2023-00004, Savannah River National Laboratory, Aiken, SC.

[38] RPP-WTP. Personal communication. 2003. "Canister Centerline Cooling Data, Revision 1, CCN: 074851, RPP-WTP," October 29, 2003.

[39] Stariha, SA and WL Ebert. 2023. *Durability Assessments of Quenched and Slow-Cooled Iron Phosphate Waste Form Materials*. ANL/CFCT-23/24, Argonne National Laboratory, Lemont, IL.

[40] Riley, BJ, S Chong, M Peterson, and ET Nienhuis. 2023. *Aluminophosphate Waste Forms for Immobilizing Cations from Electrochemical Salt Wastes*. PNNL-33906, Pacific Northwest National Laboratory, Richland, WA.

[41] Tolman, DD and BJ Riley. 2023. *Conceptual Design of a Salt Dechlorination and Vitrification Apparatus (DeVA)*. INL/RPT-23-72319, PNNL-34755, Idaho National Laboratory, Idaho Falls, ID.

[42] Stariha, SA and WL Ebert. 2023. *Corrosion Tests with Phosphate-Based Materials Made at Clemson University*. ANL/CFCT-22/52, Argonne National Laboratory, Lemont, IL.

[43] Marcial, J, S Chong, BJ Riley, RK Brow, JD Vienna, CW Kim, and M Tang. 2024. *Bonding Environments and Radiation Stabilities of Phosphate Glasses*. PNNL-35754, Pacific Northwest National Laboratory, Richland, WA.

[44] Kalahe, J, TS Mahadevan, X Lu, JD Vienna, BJ Riley, and J Du. 2024. "Insights on the structure and properties of sodium iron phosphate glasses from molecular dynamics simulations." *Journal of Nuclear Materials* **594**:155004.

[45] Hegde, VI, M Peterson, S Allec, X Lu, T Mahadevan, T Nguyen, J Kalahe, J Oshiro, R Seffens, E Nickerson, J Du, BJ Riley, JD Vienna, and JE Saal. 2024. "Towards Informatics-Driven Design of Novel Nuclear Waste Forms." *Digital Discovery* **3**(8):1450–1466.

[46] Du, J, J Kalahe, JD Vienna, and BJ Riley. 2024. "Structure and structure-property relationship in sodium iron phosphate glasses from Molecular Dynamics Simulations and QSPR analysis." *Physics and Chemistry of Glasses: European Journal of Glass Science and Technology Part B*.

[47] Chong, S, BJ Riley, X Lu, J Du, T Mahadevan, and V Hegde. 2024. "Synthesis and properties of anhydrous rare-earth phosphates, monazite and xenotime: a review." *RSC Advances* **14**(27):18978–19000.

[48] Chong, S and BJ Riley. 2024. "Compositional effects on the chemical durabilities of aluminophosphate glasses: A review." *Journal of Non-Crystalline Solids: X* **21**:100205.

[49] Evarts, JS and BJ Riley. 2024. *Completion of Milestone M4FT-24PN030104046 "Support ANL-led efforts towards dechlorinated waste forms"*. PNNL-SA-201277, Pacific Northwest National Laboratory, Richland, WA.

[50] Ebert, WL, G J.E., SA Stariha, JS Evarts, and BJ Riley. 2024. *Effect of Added Borosilicate Glass on Iron Phosphate Waste Form Material Durability*. ANL/CFCT-24/20, Argonne National Lab, Lemont, IL.

[51] Evarts, JS, HS Werth, BJ Riley, K Carlson, and MF Simpson. 2025. "Phosphate-Based Approaches for Dechlorination and Treatment of Salt Waste from Electrochemical

Processing of Used Nuclear Fuel: A Perspective on Recent Work." *ACS Omega* **10**(43):50773–50794.

[52] Werth, H, J Beland, P Murray, D Liang, L Sharpless, J Evarts, C Lonergan, BJ Riley, M Simpson, and K Carlson. 2025. "Evaluation of Processing Conditions for the Reduction of Electrochemical Salt Waste Using Phosphate-Based Dechlorination." *ACS ES&T Engineering*.

[53] Bai, J, HS Werth, BJ Riley, and M Peterson. 2025. *Evaluating High-Halide Waste Form Options for Salt-Based Nuclear Waste Simulants*. PNNL-38197, Pacific Northwest National Laboratory, Richland, WA.

[54] Riley, BJ and JD Vienna. 2025. *Technoeconomic Analysis for Evaluating Nuclear Salt Waste Form Technologies*. PNNL-37219, Pacific Northwest National Laboratory, Richland, WA.

[55] Werth, HS, K Carlson, J Beland, P Murray, D Liang, L Sharpless, BJ Riley, M Simpson, and C Lonergan. 2025. *Developments in Processing Criteria for Iron Phosphate Waste Form Design for Treating Electrorefiner Salt Wastes*. PNNL-38243, Pacific Northwest National Laboratory, Richland, WA.

[56] Werth, H, P Murray, L Greiner, J Beland, C Lonergan, B Riley, and K Carlson. 2026. "Evaluation of Iron-Phosphate Glass–Ceramic Waste Form for Electrorefiner Salt Waste Simulant Dechlorinated With Phosphoric Acid." *International Journal of Ceramic Engineering & Science* **8**(3):e70051.

[57] Carlson, K, C Lonergan, and BJ Riley. 2025. *Final Report: Investigation into the processing parameters of phosphate-based dehalogenation for chloride-based waste salt*. DE-NE0009317, University of Nevada, Reno, Reno, NV.

[58] Chong, S, BJ Riley, M Bowden, JA Silverstein, and NL Brown. 2025. *Synthesis and Crystal Structures of Alkali (Na, Rb, Cs) Iron Phosphate Crystals*. PNNL-SA-210872, Pacific Northwest National Laboratory, Richland, WA.

[59] Liao, Y, E Schneiderlochner, and WL Ebert. 2026. *Corrosion Durability of Phosphate-Based Waste Forms*. ANL/CFCT-25/43, Argonne National Laboratory, Lemont, IL.

[60] Peterson, M, BJ Riley, X Lu, KH Yano, S Mukhopadhyay, II Leavy, EK Nickerson, RJ Seffens, J Du, KD Miller, and JE Saal. 2025. "Glass-Bonded Monazite Waste Forms for Lanthanide and Actinide Immobilization: From Theoretical Design to Scale-Up Production and Characterization." *ACS Omega* **10**(30):33524–33535.

[61] Greiner, LL, K Melenbrink, H Werth, BJ Riley, K Carlson, and C Lonergan. 2026. "Process Effects and Structural Analysis on Phosphate Intermediates during Dechlorination of Mixed Chloride Waste Product for Nuclear Waste Immobilization." *under review at International Journal of Applied Glass Science*.

[62] McGuire, P, B Riley, J Amoroso, J Bussey, S Soudani, J McCloy, and K Brinkman. 2026. "Structural, Chemical, and Thermal Characterization of Novel Tin Fluorophosphate Nuclear Salt Waste Forms." *submitted to Journal of Non-Crystalline Solids*.

[63] Oshiro, J, S Choi, HS Werth, X Lu, JD Vienna, BJ Riley, J Ferrer, L El Khoury, MK Cragin, JL George, M Torres, JS Evarts, VL Augustine, E Schneiderlochner, A-M Popa, Y Liao, and WL Ebert. 2026. *Organic Acid Dehalogenation and Borosilicate Glass Waste Form Testing (TARSv2)*. PNNL-39837, Pacific Northwest National Laboratory, Richland, WA.

[64] Schneiderlochner, E, A-M Popa, Y Liao, and WL Ebert. 2026. *Corrosion Tests with Developmental TARS Materials*. ANL/CFCT-26/20, Argonne National Laboratory, Lemont, IL.

[65] Chong, S and BJ Riley. 2022. "Thermal conversion in air of rare-earth fluorides to rare-earth oxyfluorides and rare-earth oxides." *Journal of Nuclear Materials* **561**:153538.

[66] Ebert, WL, BJ Riley, and SM Frank. 2017. *Test Plan for Salt Treatment and Waste Form Development*. NTRD-MRWFD-2017-000191, Argonne National Laboratory, Lemont, IL.

[67] Corning. 7056 Alkali Borosilicate Glass. Corning. 2017. Accessed at https://www.corning.com/media/worldwide/csm/documents/7056%20PI%20sheet_Letter_032017_b.pdf.

[68] Simpson, M, K Carlson, D Rappleye, J Du, J McCloy, X Guo, T Cisneros, JE Saal, BJ Riley, U Carvajal, G Peterson, G Cao, and M Gonzalez. Development of Waste Processing Methods for MCFR Fuel Salt. 2026. Accessed at https://neup.inl.gov/content/uploads/14/2026/03/2025-CFA-Summary-Abstract-IRP-25-35167.pdf.

[69] Riley, BJ. 2020. "Electrochemical salt wasteform development: A review of salt treatment and immobilization options." *Industrial & Engineering Chemistry Research* **59**(21):9760–9774.

[70] Stefanovsky, SV, OI Stefanovsky, BF Myasoedov, SE Vinikurov, SS Danilov, BS Nikonov, KI Maslakov, and YA Teterin. 2017. "The phase composition, structure, and hydrolytic durability of sodium-aluminum-(iron)-phosphate glassy materials doped with lanthanum, cerium, europium, and gadolinium oxides." *Journal of Non-Crystalline Solids* **471**:421–428.

[71] Stefanovsky, SV, OI Stefanovsky, SS Danilov, and MI Kadyko. 2019. "Phosphate-based glasses and glass ceramics for immobilization of lanthanides and actinides." *Ceramics International* **45**(7, Part B):9331–9338.

[72] Shannon, RD. 1976. "Revised effective ionic radii and systematic studies of interatomic distances in halides and chalcogenides." *Acta crystallographica section A: crystal physics, diffraction, theoretical and general crystallography* **32**(5):751–767.

[73] Moreau, F, A Durán, and F Muñoz. 2009. "Structure and properties of high Li2O-containing aluminophosphate glasses." *Journal of the European Ceramic Society* **29**(10):1895–1902.

[74] Brow, RK. 1993. "Nature of alumina in phosphate glass: I, properties of sodium aluminophosphate glass." *Journal of the American Ceramic Society* **76**(4):913–918.

[75] Brow, RK, RJ Kirkpatrick, and GL Turner. 1993. "Nature of alumina in phosphate glass: II, structure of sodium alurninophosphate glass." *Journal of the American Ceramic Society* **76**(4):919–928.

[76] El Damrawi, G, AK Hassan, and A Shahboub. 2020. "Chemical durability and structure of Al_2O_3–Ag_2O–P_2O_5 glasses." *Applied Physics A* **126**(4):1–7.

[77] Metwalli, E and RK Brow. 2001. "Modifier effects on the properties and structures of aluminophosphate glasses." *Journal of non-crystalline solids* **289**(1-3):113–122.

[78] Karabulut, M, E Melnik, R Stefan, GK Marasinghe, CS Ray, CR Kurkjian, and DE Day. 2001. "Mechanical and structural properties of phosphate glasses." *Journal of Non-Crystalline Solids* **288**(1-3):8–17.

[79] Chenu, S, U Werner-Zwanziger, C Calahoo, and JW Zwanziger. 2012. "Structure and properties of $NaPO_3$–ZnO–Nb_2O_5–Al_2O_3 glasses." *Journal of non-crystalline solids* **358**(15):1795–1805.

[80] Ebert, WL, CT Snyder, BJ Riley, and SM Frank. 2016. *Designing Advanced Ceramic Waste Forms for Electrochemical Processing Salt Waste*. FCRD-MRWFD-2016-000038, Argonne National Laboratory, Lemont, IL.

Appendix A – Additional Details about Recent Studies

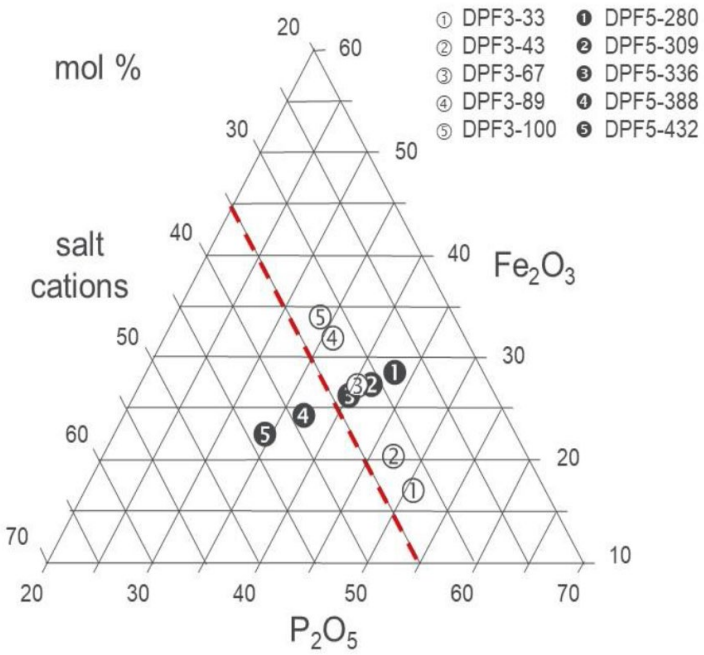

Figure A-1. Ternary diagram showing relative amounts of salt, P_2O_5, and Fe_2O_3 used to make DPF materials represented by the equivalent glasses, in mol%. This figure comes from [35].

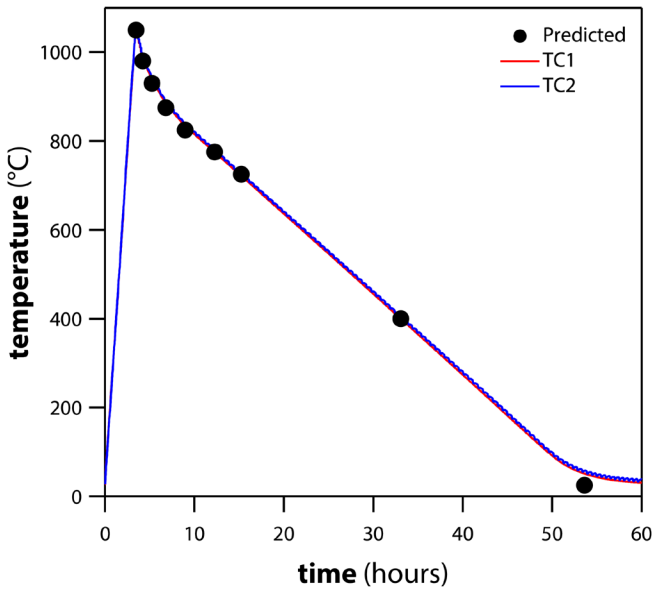

Figure A-2. Canister centerline cooling (CCC) curve mimicking a high-level waste canister along with thermocouple measurements taken during the curve in the study by Riley et al. [30].

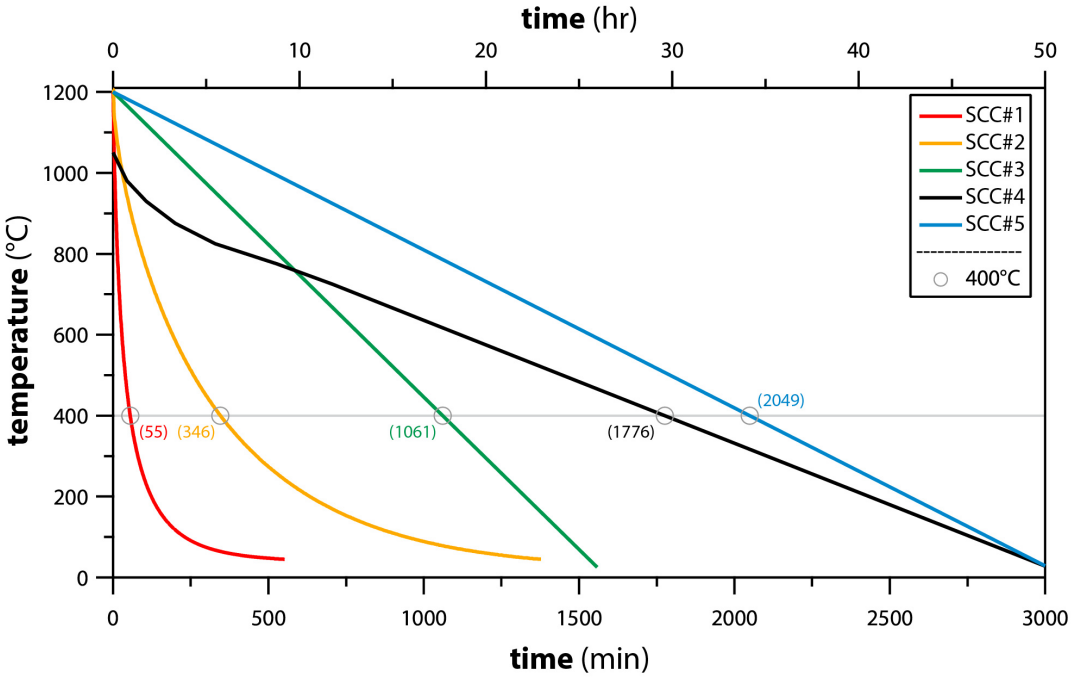

Figure A-3. SCC# cooling curves evaluated for processing DPF5-336. Note that SCC#1 is only a theoretical curve while SCC#2, SCC#3, and SCC#5 were the focus of the current study. SCC#4 was run on DPF5-336 in a separate study and the results can be found in a document published previously. This figure comes from Riley et al. [34].

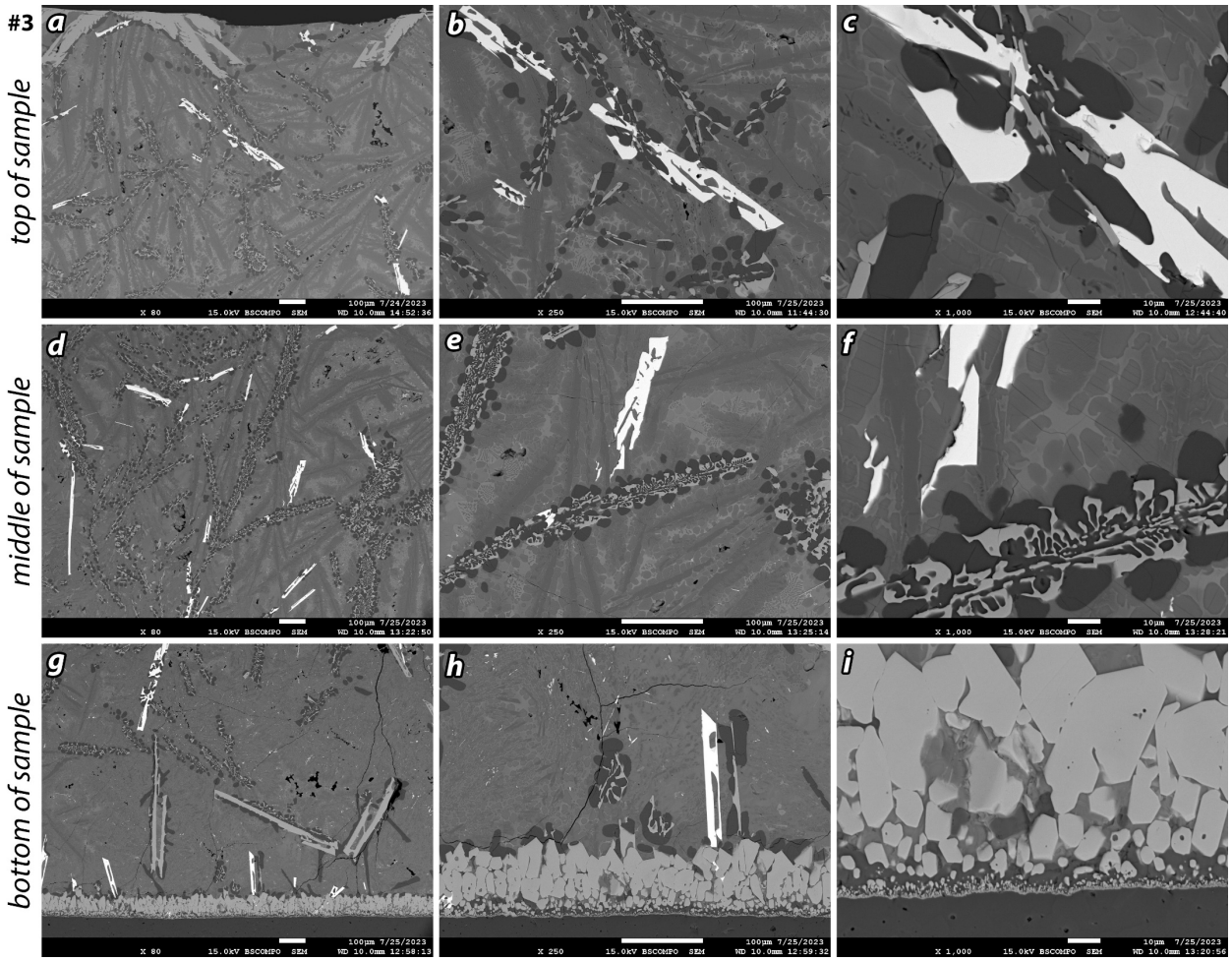

Figure A-4. SEM micrographs of SCC#3 showing the (a-c) top, (d-f) middle, and (g-i) bottom regions at magnifications of (a,d,g) 80×, (b,e,h) 250×, and (c,f,i) 1k×. This data comes from the study by Riley et al. [34].

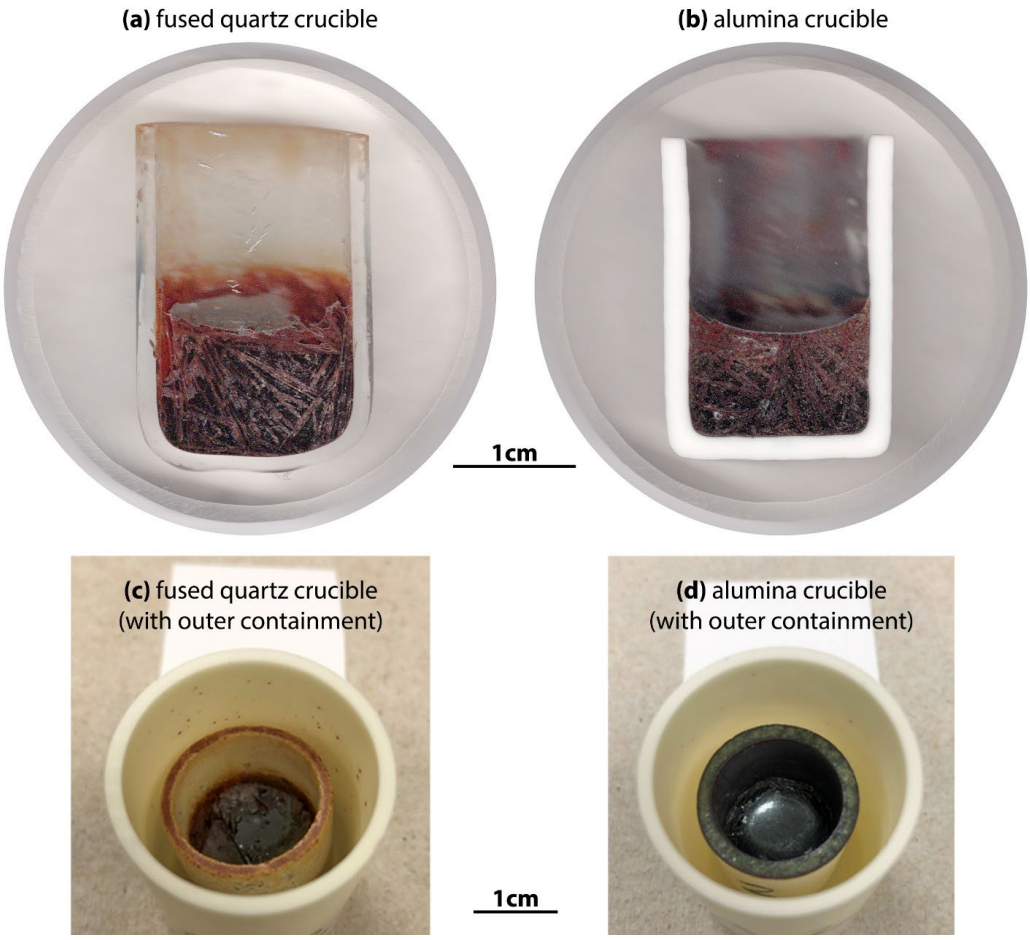

Figure A-5. Pictures of DPF5-336 samples following CCC treatments in (a,c) a fused quartz crucible and (b,d) an alumina crucible including (a,b) cross-sectioned views in resin and (c,d) the samples prior to cross-sectioning while still in the original crucibles and secondary containment crucibles. This figure comes from Riley et al. [36].



Figure A-6. Pictures of the four glasses produced and compared within the aluminophosphate study [40].

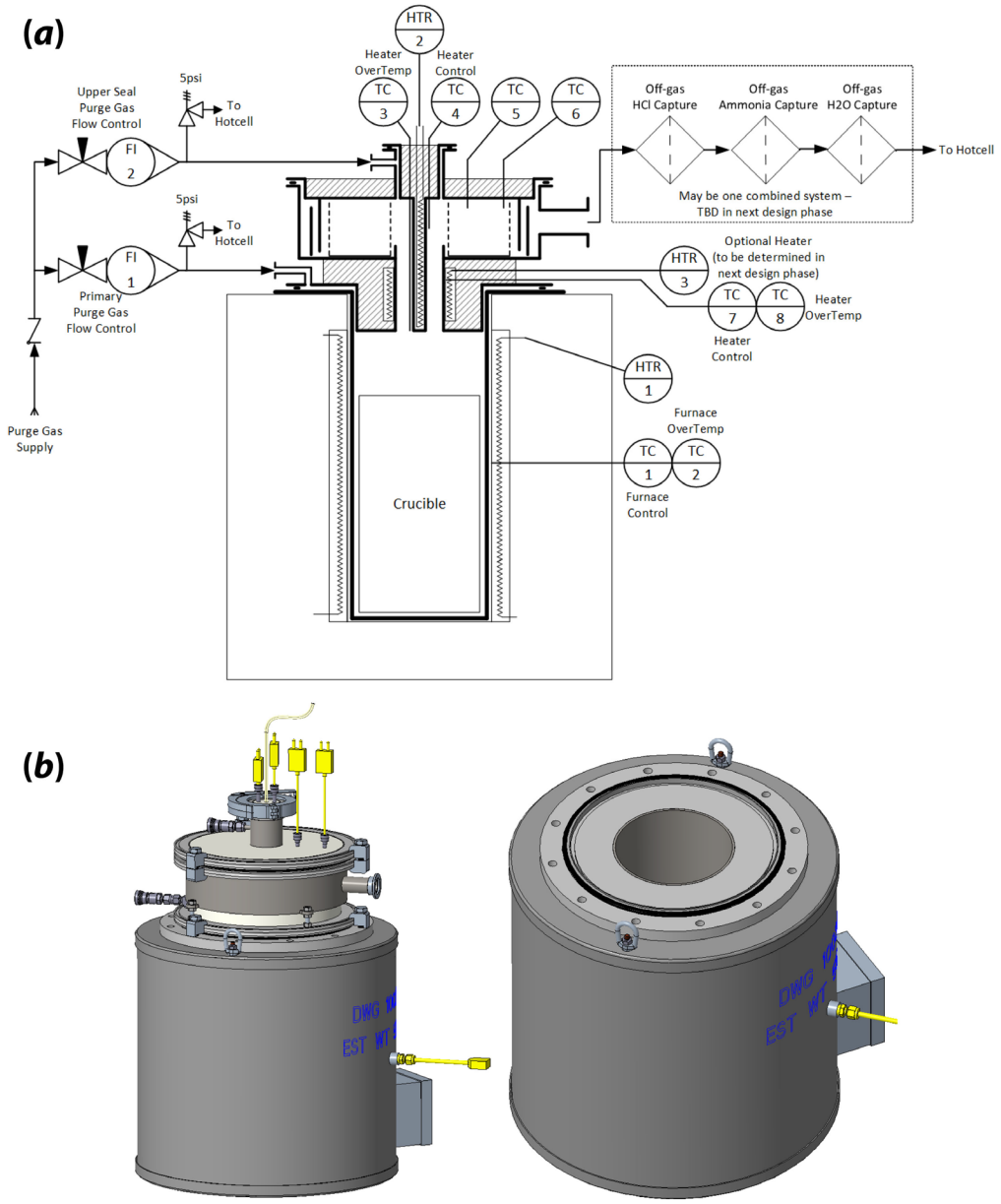

Figure A-7. (a) Conceptual process and instrumentation diagram for the DeVA and (b) the conceptual model shown (left) with the condenser and (right) without the condenser. This graphic comes from Tolman and Riley [41].

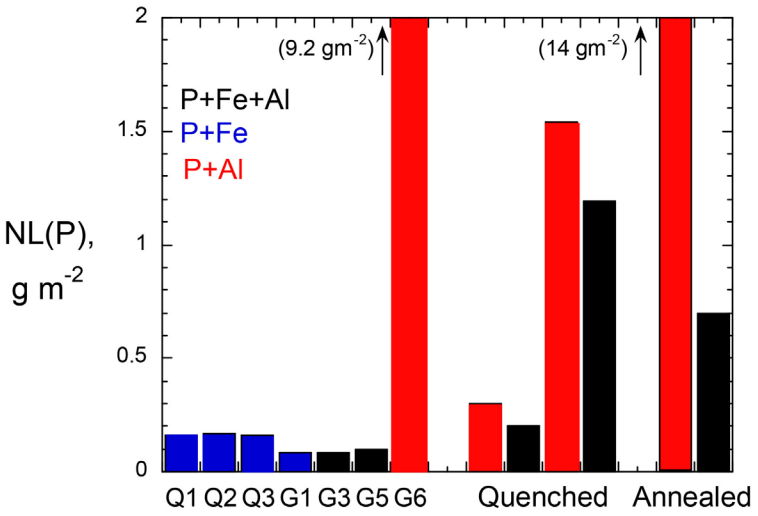

Figure A-8. Summary of ASTM C1285 tests performed with DPFRQ materials (Q1, Q2, Q3, G1) [32, 36, 40], iron aluminophosphates (G3, G5) [40], and aluminophosphate glass (G6), along with calculated values of quenched and annealed glass from other studies [70, 71]. This figure comes from Stariha et al. [39].

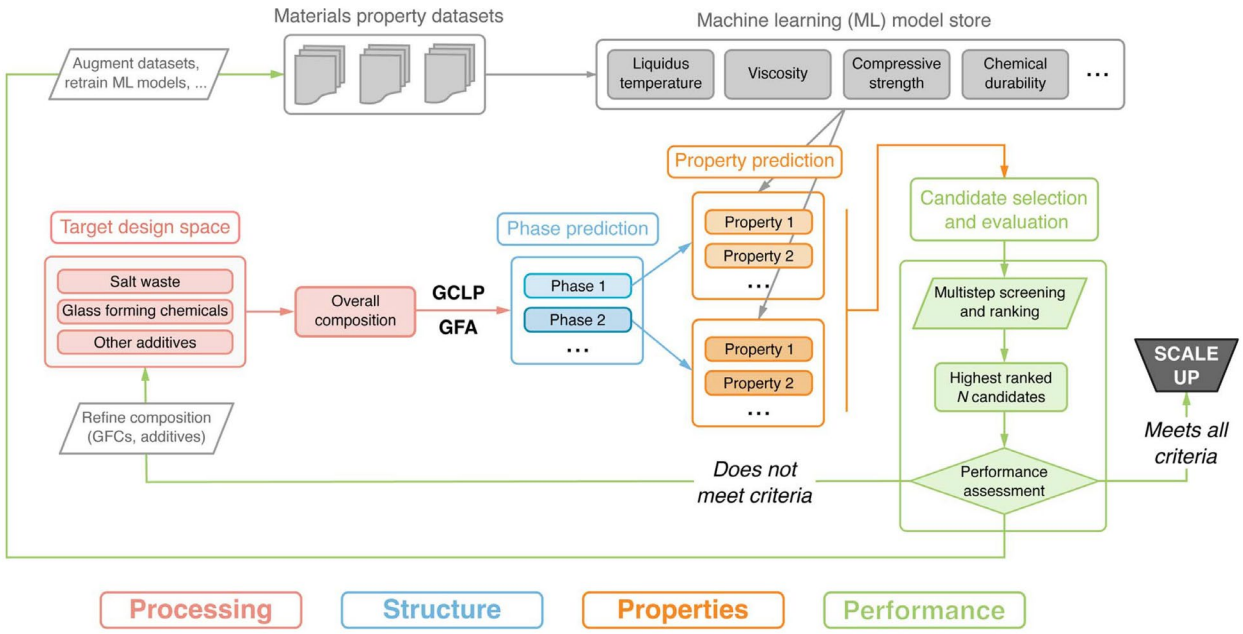

Figure A-9. A sample sequential learning driven workflow for the design of novel waste forms, informed by the underlying system design chart. This figure comes from Hegde et al. [45].

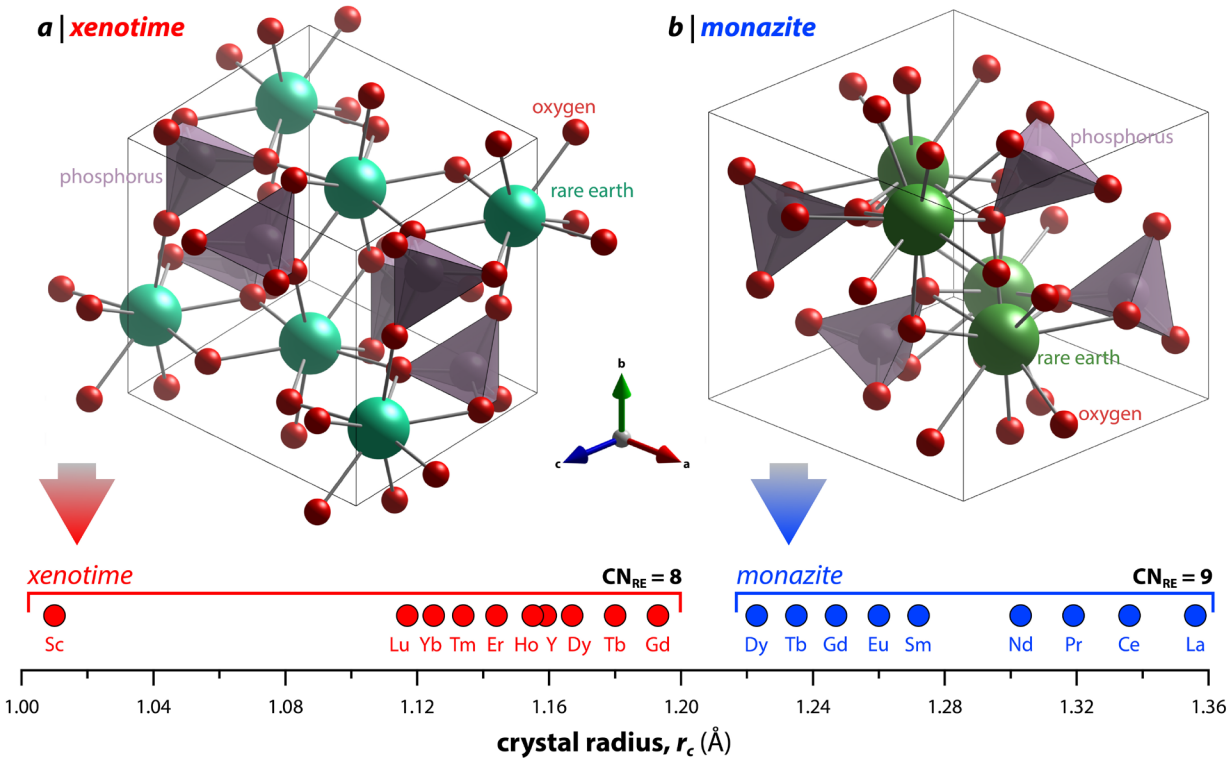

Figure A-10. Illustration showing the relationship of (a) xenotime and (b) monazite structures of *RE*PO_4 to the *RE* crystal radii (r_c) from Shannon [72]. $LuPO_4$ (ICSD 46792) and $LaPO_4$ (ICSD 46788) were used to create the (a) xenotime and (b) monazite unit cell structures, respectively. This figure comes from Chong et al. [47].

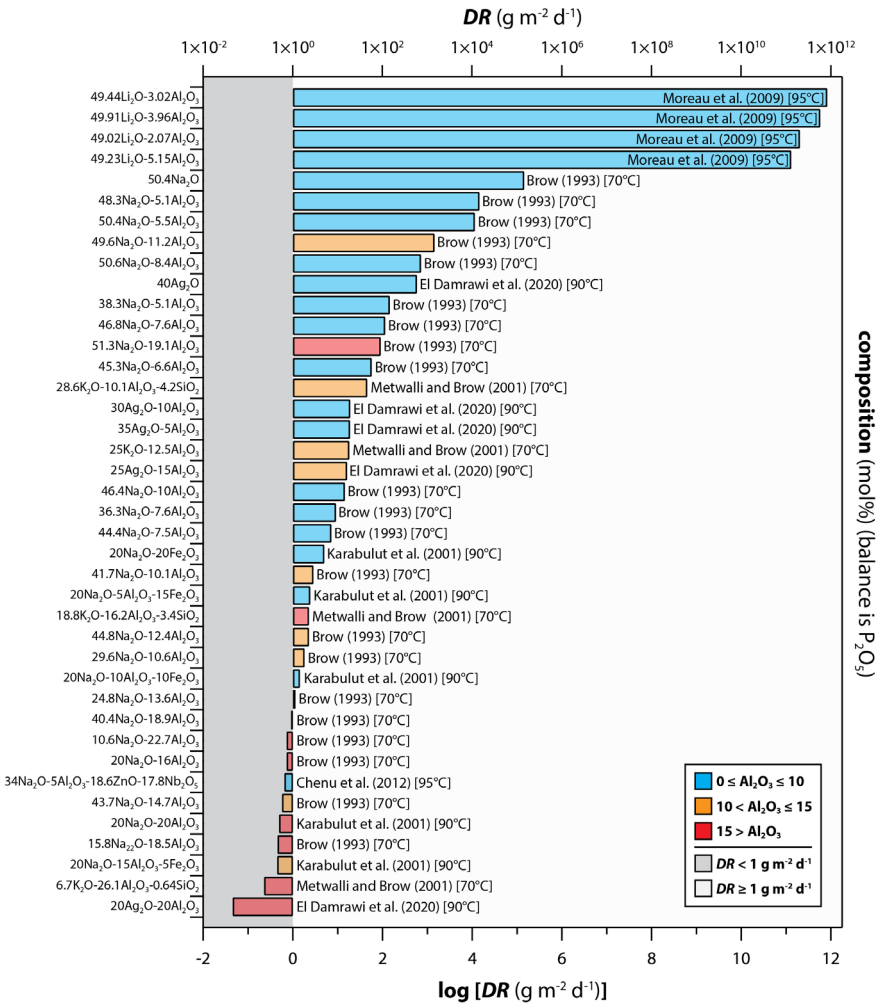

Figure A-11. Dissolution rate (DR) of M_2O-Al_2O_3-P_2O_5 glasses from various studies [73-79]. The listed compositions of glasses are balanced with P_2O_5. This figure comes from Chong and Riley [48].

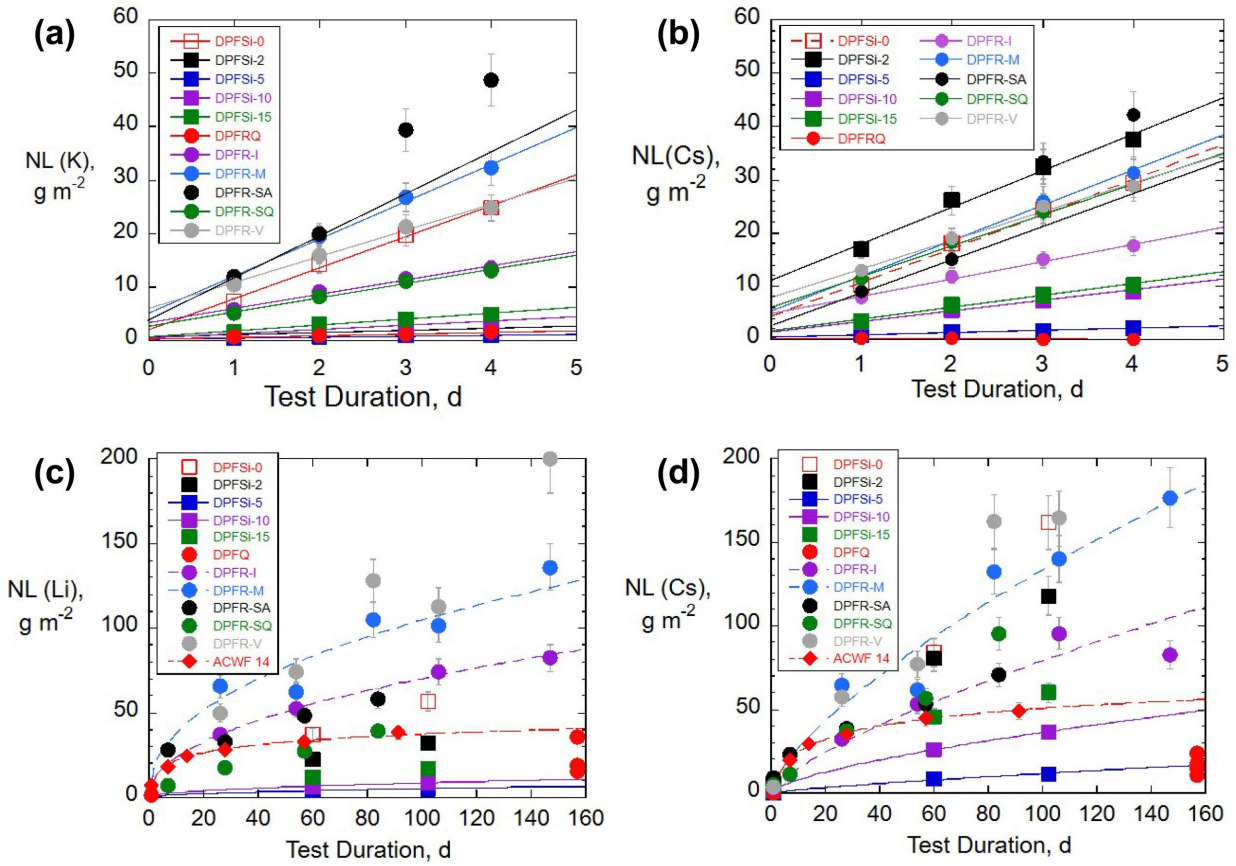

Figure A-12. Comparisons of (a,b) ASTM C1308 and (c,d) ASTM C1220 leaching test results for a range of electrochemical waste forms, including the DPF5-336 reference material (DPFR) in quenched form (DPFRQ); DPFR cooled at different rates (i.e., DPFR-M is moderately cooled; DPFR-I is intermediately cooled); CCC-cooled in alumina (DPFR-SA) and fused quartz (DPFR-SQ); the 14 mass% advanced ceramic waste form (ACWF-14) from a separate study [5, 80]; along with phosphosilicate glasses (DPFSi) made with 2.5–15 mass% NBS-3 from a separate study [51]. These figures come from Ebert et al. [50].

Table A-1. Process comparisons between starting with ADP or H_3PO_4 for dechlorination and vitrification processes. This comes from Werth et al. [52] and is reprinted with permission.

Criteria	Category	$NH_4H_2PO_4$(ADP) + salt	H_3PO_4 + salt
Overview	General reaction	Mixture of ADP and salt, which melts ~ 200 °C, and metal cations are incorporated into a phosphate glass matrix as phosphate and oxides.	Aqueous slurry of 14.615 M H_3PO_4 and salt, which increase in viscosity with temperature as water evolves and metal chlorides are incorporated into a phosphate glass matrix.
Dechlorination Process	Salt types	Dechlorination can be performed on simple (no surrogate FPS) and complex (includes surrogate FPs) salt mixtures.	
	Heating profile	Continuous ramping (5–10 °C/min) and/or isothermal holds of 1 h at each 100 °C up to 600 °C.	
	Starting temperature	Dechlorination begins ~200 °C.	Dechlorination beings immediately upon mixing H_3PO_4 with the salt mixture.
	Decomposition products	ADP decomposes at ≈190 °C to form NH_3 and H_2O.	Release of H_2O and HCl peaks at ~100 °C, corresponding with the boiling temperature of water.
	Residual Cl in air atmosphere	~1 wt % residual chlorine after dechlorination of simple salt (48LiCl-33KCl-19NaCl mol %) in air.	Very low residual chlorine after dechlorination of simple salt (48LiCl-33KCl-19NaCl mol %) in air.
	Residual Cl in Ar atmosphere	Dechlorination in argon has not been tested.	Very low residual chlorine after dechlorination of simple salt (48LiCl-33KCl-19NaCl mol %) in argon.
	Main off-gas byproducts	NH_4Cl(s,g), H_2O(l,g), HCl(l,g), and NH_3(l,g).	HCl(l,g) and H_2O(l,g).
	Solid condensates	Gaseous NH_4Cl readily condenses ≈200–260 °C, potentially providing a solid byproduct.	No solid condensates.
	Dechlorinated product	Phosphate glass containing salt cations in the form of phosphates or oxides.	
Waste Form Process	Stabilization	Dechlorinated product must be mixed with additional components (Fe_2O_3, Al_2O_3) and vitrified at higher temp. (≥1000 °C) for increased chemical durability.	
	Slow cooling	Must be assessed as the vast majority were quenched and glass forming ability is unknown.	
Safety	Chemical hazards	Release of acidic and corrosive vapors.	
	Foaming and volume expansion	Extreme bubbling occurs during processing (<300 °C).	Reactions begin as soon as precursor is mixed with salt with moderate bubbling during initial heating (<300 °C).
	Hazardous byproducts	Reactions between nitrogen-containing compounds and halide compounds can produce dangerous byproducts.	Requires working with strong acids (i.e., H_3PO_4).
Crucible Interactions	Best performers	Alumina, silica, and glassy carbon crucibles have been shown to have little to no interaction with the sample during dechlorination of salt (<1.0 wt % of crucible material in the dechlorinated product).	Dechlorination in silica crucibles resulted in <0.3 wt % silica in dechlorinated product. Silica crucibles used for dechlorination of a simple salt mixture at >400 °C would frequently shatter when cooled. Crucibles used for dechlorination of ERV3 did not shatter.
	Works performers (or future work)	Processing in Ni, boron nitride (AX05, HP, ZSBN) crucibles resulted in adherence of the product to the crucible and high levels of reaction.	Interactions with alternative crucible materials has not been tested.

Table A-2. Summary of corrosion of bars in molten DPF5-336. The corroded area was determined by OM in the 13.8 mm region around the neck. Oxide depth, penetration depth, and crack depth were determined with SEM-EDS. Penetration depth includes the oxide depth. N/A = not applicable, with footnotes below the table with additional details, ID = identification. This table comes from Werth et al. [55].

Coupon Material	Atmos.	Test Time (h)	Sample ID	Corroded Area at the Neck (mm^2)	Oxide Depth (µm)	Maximum Penetration Depth (µm)	Crack Depth (µm)	Secondary Phases	Ranking
Fused quartz	Air	1	Fused quartz-Air-1h	N/A[a]	N/A[b]	150[c]	<220[d]	N/A[e]	1
		4	Fused quartz -Air-4h	N/A[a]	N/A[b]	200[c]	<300[d]		
	Argon	1	Fused quartz -Ar-1h	N/A[a]	N/A[b]	200[c]	<240[d]		
		4	Fused quartz -Ar-4h	N/A[a]	N/A[b]	200[c]	<300[d]		
Alumina	Air	1	Alumina-Air-1h	0.96	<5	N/A[f]	N/A[g]	Iron oxide[h]	2
		4	Alumina-Air-4h	N/A[i]	<5	N/A[f]	N/A[g]		
	Argon	1	Alumina-Ar-1h	1.70	<10	N/A[f]	N/A[g]		
		4	Alumina-Ar-1h	3.71	<20	N/A[f]	N/A[g]		
Monofrax K3	Air	1	K3-Air-1h	0.41	30-50	250	N/A[g]	Chromium oxide[j]	3
		4	K3-Air-4h	3.62	<100	2500	N/A[g]		
	Argon	1	K3-Ar-1h	0.37	30-50	180	N/A[g]		
		4	K3-Ar-4h	2.03	10-60	520	N/A[g]		
SS316L	Air	1	SS-Air-1h	8.90	>1000	1300	N/A[g]	Chromium oxide, Mo, Ni, P, Fe alloy[k]	4
		4	SS-Air-4h	N/A[h]	N/A[h]	N/A[h]	N/A[h]		
	Argon	1	SS-Ar-1h	14.20	<100	500	N/A[g]		
		4	SS-Ar-4h	N/A[h]	N/A[h]	N/A[h]	N/A[h]		
Inconel 693	Air	1	Inconel-Air-1h	N/A[i]	>1000	100	N/A[g]	Cr and Al oxides, Ni and P alloy[k]	5
	Argon	1	Inconel-Ar-1h	28.34	>1000	100	N/A[g]		

[a]The material loss at the neck region of fused quartz samples could not be determined with optical microscopy due to a combination of surface cracking, DPF5-336 deposits, and lack of a distinct sample edge due to the optical clarity of the material; however, material loss due to degradation appeared to be negligible. [b]No oxide layer was observed in fused quartz samples. [c]Maximum penetration depth in fused quartz bars occurred in cracks. [d]Cracks were approximately equal in depth over the entire surface of the fused quartz bar exposed to DPF5-336. [e]Fused quartz bars did not have secondary phases composed of corroded material. [f]Penetration of DPF5-336 components into the bulk of alumina bars was not observed. [g]Sample did not have cracks. [h]The iron oxide layer was homogeneous in both composition and thickness over the surface of the bar. [i]The area corroded in the neck region could not be determined due to the extensive material loss in this sample that caused the sample to separate into two sections during preparation. [j]Chromium oxide and DPF5-336 formed a heterogeneous layer that varied in thickness over the surface of the bar. [k]Secondary phases formed a heterogeneous corroded layer that varied greatly both in composition and thickness depending on the location on the bar.

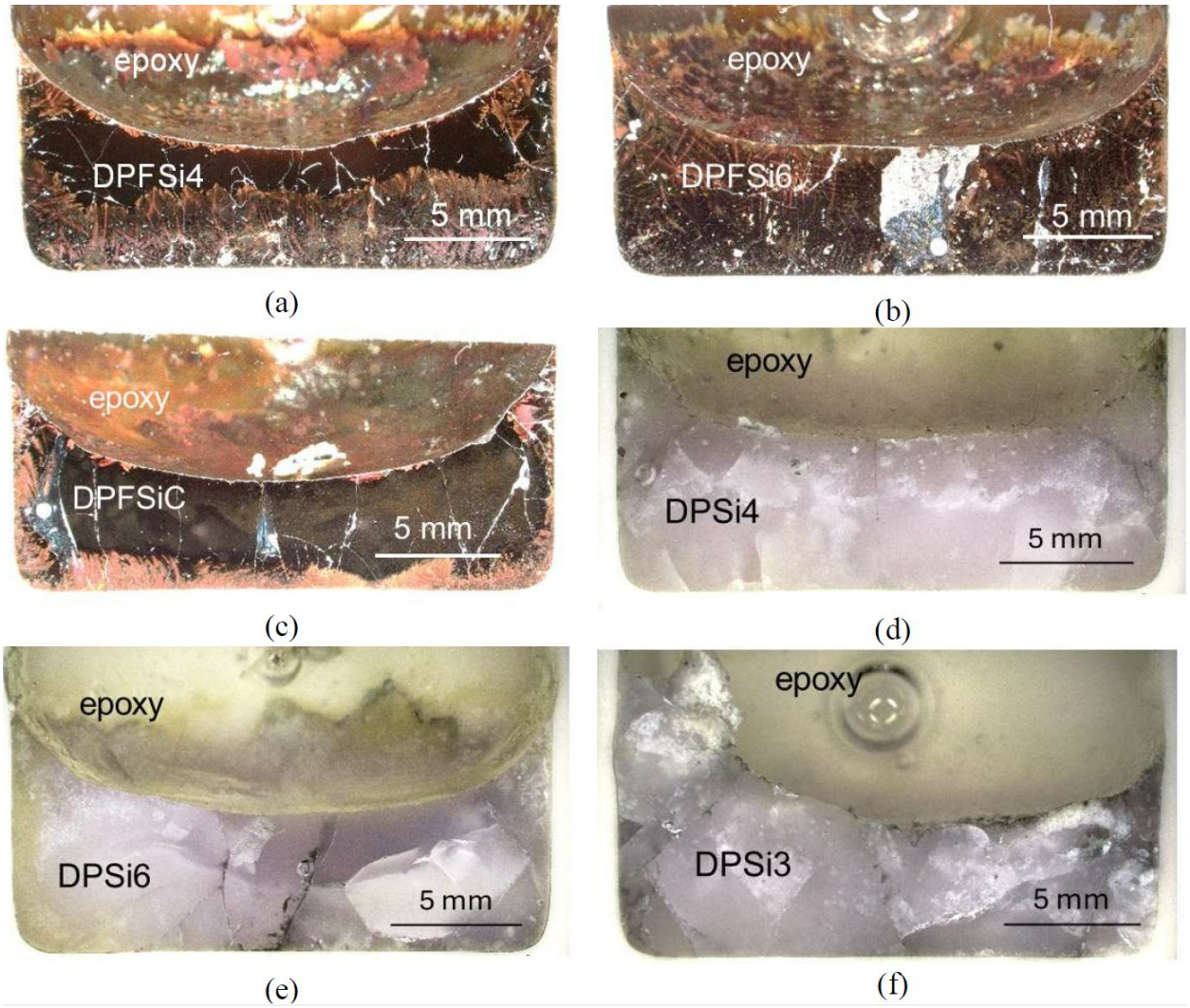

Figure A-13. Optical micrographs of cross-sectioned materials (in epoxy) used in tests, including (a-c) Fe_2O_3-containing samples with 5 mass% silicate glass of (a) DPFSi4 (NBS-4), (b) DPFSi6 (NBS-6), and (c) DPFSiC (Corning C7056) and (d-f) glasses without Fe_2O_3 and with 15 mass% silicate glass of (d) DPSi4 (NBS-4), (e) DPSi6 (NBS-6), and (f) DPSi3 (NBS-3).

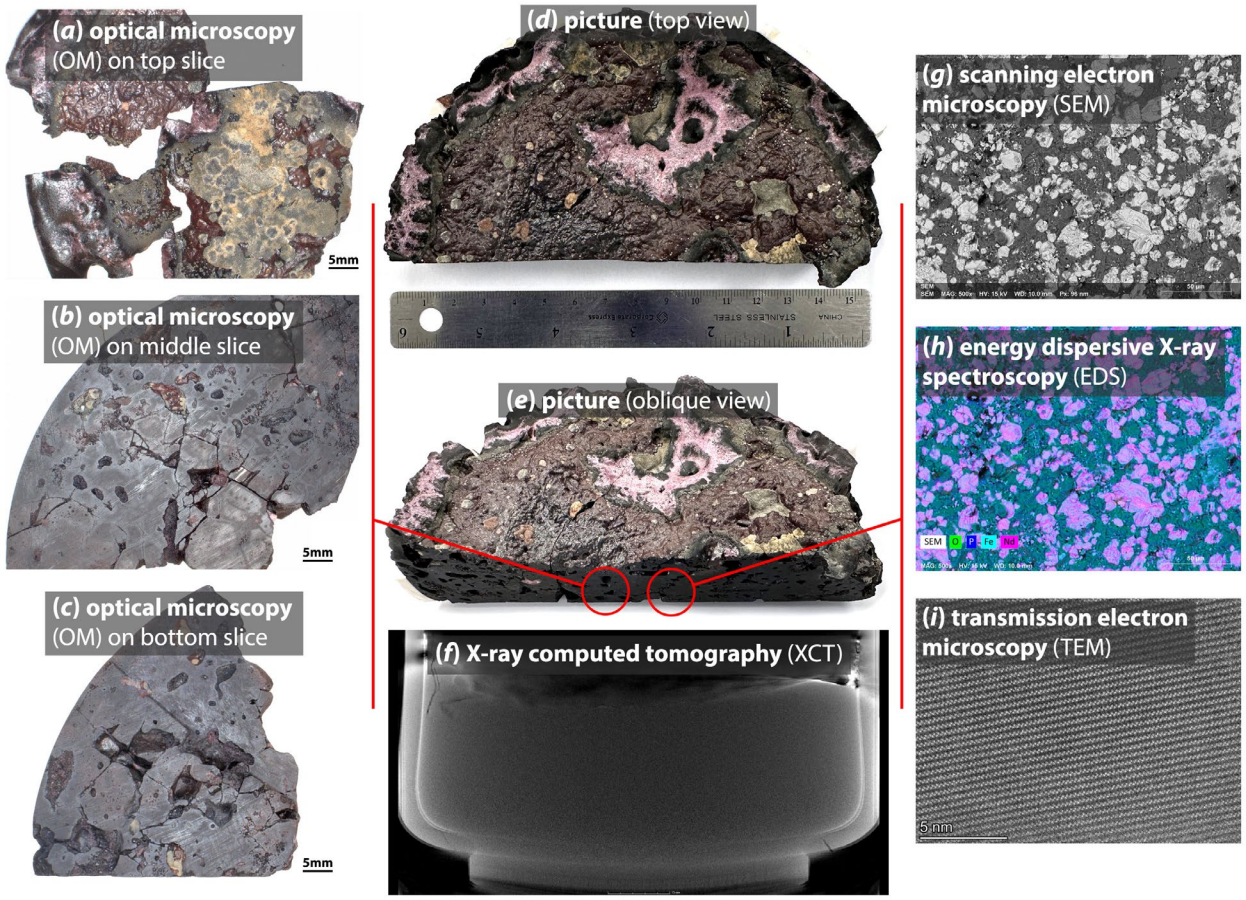

Figure A-14. Summary of results from scale-up sample 37Nd-1600g showing (a−c) cross-sectional views of the slices from the full sample, (d,e) pictures the full sample at different angles (top down and oblique views, respectively), (f) X-ray computed tomography image of the sample still within the crucible, (g) SEM micrograph, (h) EDS elemental overlay, and (i) scanning transmission electron micrograph of the sample. This figure comes from Peterson et al. [60].

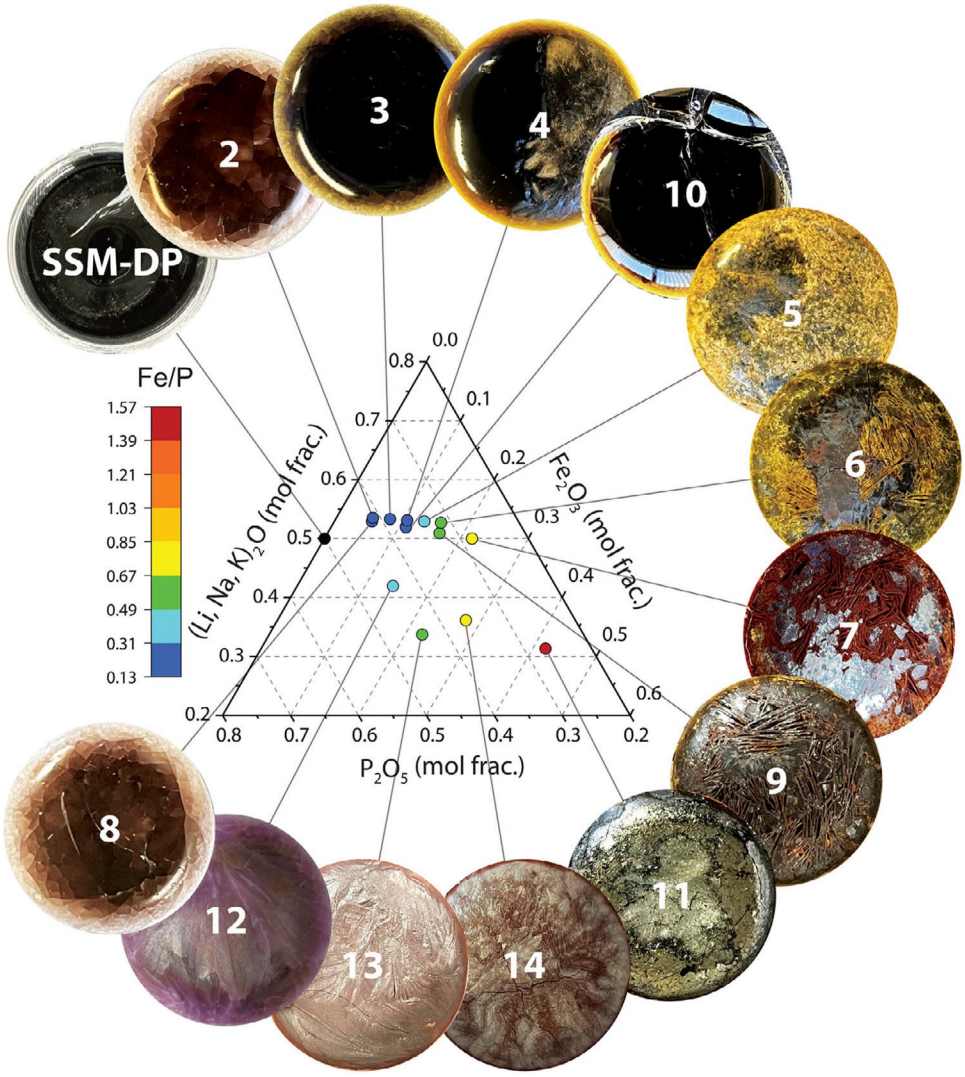

Figure A-15. The target compositions (mol fraction) of glasses produced in the study by Werth et al. [56].

Appendix B – Road Map Categories

This section provides and overview of the sections with Table 1-1 of the original road map report from Riley et al. [1]. The major categories include **Waste Composition** (see Table B-1), **Matrix and Additives** (see Table B-2), **Waste Processing** (see Table B-3), **Waste Form Properties** (see Table B-4), **Waste Form Acceptance** (see Table B-5), and **Waste Form Performance** (see Table B-6). For clarification, here are some additional details/abbreviation that show up within these tables: ADP = $NH_4H_2PO_4$; BS = borosilicate (glass); CCC = canister centerline cooling; CTE = coefficient of thermal expansion; DHP = $(NH_4)_2HPO_4$; DPF = dehalogenated phosphate forms; ER = electrorefiner (salt); MSR = molten salt reactor; NRC = Nuclear Regulatory Commission; OR = oxide reduction (salt); WF = waste form; WL = waste loading.

B.1 Waste Composition Evaluation

Table B-1. Summary of **Waste Composition** areas of research needed, potential issues for pursuing these areas of research, the current state of the art, as well as identified gaps and possible ways to fill those gaps (more information is provided in subsequent sections for each topic area).

Issues	Current Status	Approaches to Fill Gaps
The range of ER and OR salt waste compositions that will ultimately be produced has not been clearly defined. The waste composition and characteristic ranges are needed to support waste form, process design, and disposal qualification activities.	Current electrochemical salt wastes are dominated by LiCl (OR) and LiCl/KCl eutectic mixtures (ER), and include fission products, other fuel constituents, such as sodium, and trace actinides. The salts are anticipated to be used until reaching some limiting factor that may be related to the physical properties of the salt (e.g., liquidus temperature) the decay heat management of salt waste forms, impacts on product purity, or other limiting factors.	Electrochemical process development, waste form design, waste processing, and disposal requirements need to be developed concurrently due to the potential feedback effects of each technology component on the others. By doing so, the ranges of key waste component concentrations and waste characteristics will be refined.
Several chloride and fluoride salt mixtures are being considered by MSR designers. For MSRs, salt compositions vary depending on vendor design and operating strategy. The range of halide salt wastes generated from prototypical MSRs are needed.	Several different fuel/coolant salt compositions have been proposed by MSR vendors. These include both chloride-based salts (primarily for fast reactors) and fluoride-based salts (primarily for thermal reactors). The salt constituents, the fission and activation products, and the fuel burnup prior to processing differ.	Work with other organizations within DOE-NE and the potential MSR vendors to develop a database of fuel compositions and characteristics. Select from the list example salt composition for use in waste form and process development activities.

B.2 Matrix and Additive Evaluation

Table B-2. Summary of **Matrix and Additives** areas of research needed, potential issues for pursuing these areas of research, the current state of the art, as well as identified gaps and possible ways to fill those gaps (more information is provided in subsequent sections for each topic area).

Issues	Current Status	Approaches to Fill Gaps
Alkali- and alkaline earth-phosphate glasses, *without glass-forming additives*, are not sufficiently durable to serve as a waste form. Additive such as Fe_2O_3 and Al_2O_3 can be used to improve chemical durability but require higher-temperature vitrification in a separate processing step. Some composition regions are prone to crystallization and form phases that may be detrimental to processing or performance. Adequate compositions are required for phosphate glasses that are processable and durable with dehalogenated salt wastes as major components of the glasses.	Iron phosphate and aluminophosphate glasses have been formulated and tested for several nuclear waste streams in the U.S. and abroad. Several iron-phosphate glass compositions were developed specifically for dehalogenated ER salt waste. To the best of the authors knowledge, phosphate glasses were not developed for a range of the dehalogenated salt wastes generated from ER, OR, and MSRs.	Design and test phosphate-based glasses with a range of different salt compositions, additives, and waste loadings to survey the boundaries of acceptable glass formation.
Nuclear waste glass design, qualification, and process control all rely heavily on the ability to predict glass properties as functions of key composition and processing related parameters. Few if any such models are available for iron-phosphate based glasses.	Models available for iron-phosphate glass properties are few (e.g., density, CTE) and are aimed at Hanford tank waste compositions rather than dehalogenated salt wastes.	Develop glass property-composition data and associated models over the range of likely glass compositions. These data and models should include properties such as durability response, processability related properties, and glass forming ability.

B.3 Waste Processing Evaluation

Table B-3. Summary of **Waste Processing** areas of research needed, potential issues for pursuing these areas of research, the current state of the art, as well as identified gaps and possible ways to fill those gaps.

Issues	Current Status	Approaches to Fill Gaps
A single-step process is preferred for simplicity and scale-up, but the system does not operate as desired during single-step scoping tests.	Scoping tests with 1-step vs 2-step tests show that the 2-step dehalogenation-vitrification process is more effective for Cl-based salts.	Evaluate alternative options for making the 1-step process work effectively.
Reactant optimization for different chloride salt wastes (e.g., H_3PO_4 vs ADP; different Fe additives).	Preliminary tests with ADP and H_3PO_4 have shown some success for a two-stage process.	Evaluate different phosphate precursors for different chloride salt streams.
Dehalogenation and immobilization reactions require evaluation of fluoride salts.	It is theoretically possible to dehalogenate fluoride based MSR salts using phosphate precursors, it has not yet been demonstrated.	Perform initial dehalogenation tests with H_3PO_4 and ADP. Evaluate other potential reactions.
Integrated process tests are needed to determine adequacy of materials flows and determine partitioning between process streams.	No integrated process tests have yet been performed.	Perform laboratory/bench-scale integrated process tests, develop reaction rates and process flow sheets. Separate tests may need to be done for waste forms made with different salt types.
Evaluate off-gas stream compositions, treatment requirements, and treatment methods.	Off-gas compositions are unknown and potentially problematic. For example, $HF_{(g)}$ can be generated with fluoride salts, which will attack most glassware; chlorides: off-gases require neutralization; iodides: N-I compounds (e.g., NI_3, NH_4I_3) are contact explosives so ADP or DHP are not good choices for I-containing salts.	Evaluate off-gas generation, neutralization, and need for recycling and treatment. Develop and test off-gas treatment/recycle methods.
Process ranges are not determined.	No data on processing ranges available (temperature, time, composition, gas flow, etc.).	Perform integrated process tests over range of key processing parameters. Determine processing success boundaries and develop process models. (may need to be done for different salt types).
Process equipment remote operation and maintenance.	No process equipment yet developed.	Evaluate methods to remotize process equipment and demonstrate effective hands-off operations and control.
Scale-up testing is required to evaluate overall system performance (e.g., process rates, component partition factors)	No scale-up data exists.	Scale-up integrated process tests from laboratory-scale to pilot scale (may need to be done for different salt types).
Determine process equipment lifetime and replacement requirements.	No process equipment yet developed. Salt waste streams and their byproducts are highly corrosive, adding challenges to equipment design and materials lifetime.	Study materials corrosion processes at laboratory scale. Design equipment and test equipment lifetime thought scaled testing of individual components and integrated systems.
Determine safety concerns from processes required to make iron phosphate waste forms.	Current precursors used for iron phosphate waste form production evolve toxic gases, e.g., NH_3, HCl, HF.	Determine how/if these hazards can be effectively mitigated.
Safeguards and materials accountancy.	Some radionuclides may need to be tracked throughout process for accountancy.	Regulations established by NRC.

B.4 Waste Form Property Evaluation

Table B-4. Summary of **Waste Form Properties** areas of research needed, potential issues for pursuing these areas of research, the current state of the art, as well as identified gaps and possible ways to fill those gaps (more information is provided in subsequent sections for each topic area).

Issues	Current Status	Approaches to Fill Gaps
Waste glasses tend to crystallize during slow cooling after melting.	Few data exist for canister centerline cooling (CCC) treatments of phosphate glasses with relevant ER/MSR salt waste compositions.	More data are needed to evaluate properties of CCC-treated WFs including what crystals form and how they affect glass properties of interest.
Crystallization can occur during CCC, which can lead to cracking and embrittlement of the WF.	Little is known about how CCC treatments affect crystallization in these WFs, and therefore, chemical and physical robustness.	Evaluate the chemical and physical robustness of CCC-treated phosphate glasses.
Few studies exist in the literature on the thermal stability of phosphate glasses (including compositions expected from these salt streams).	Little is known about the thermal stability of these glasses.	Evaluate thermal stability of these glasses.
Few studies exist in the literature on the radiological stability of phosphate glasses (including compositions expected from these salt streams).	Little is known about the radiological stability of these glasses.	Evaluate radiological stability of these glasses.
Determine if waste form should remain in crucible and be placed into a canister or be poured into a canister. Determine if radiation dose and heat from waste form with high waste loading require a special storage facility or longer cooling times before transport and disposal.	Only generic thermal properties and limits of iron phosphate glasses are known.	Determine thermal properties and thermal limits of iron phosphate waste forms.

B.5 Waste Form Acceptance Evaluation

Table B-5. Summary of **Waste Form Acceptance** areas of research needed, potential issues for pursuing these areas of research, the current state of the art, as well as identified gaps and possible ways to fill those gaps (more information is provided in subsequent sections for each topic area).

Issues	Current Status	Approaches to Fill Gaps
The chemical durabilities of phosphate glasses vary significantly with minor differences in composition.	Literature shows that targeting an O:P molar ratio of 3.4–3.5 and maximizing Fe:P ratios improve chemical durability of Fe-P-O glasses.	Evaluate consistency and regulatory acceptability for phosphate glasses made with different salt waste streams.

B.6 Waste Form Performance Evaluation

Table B-6. Summary of **Waste Form Performance** areas of research needed, potential issues for pursuing these areas of research, the current state of the art, as well as identified gaps and possible ways to fill those gaps (more information is provided in subsequent sections for each topic area).

Issues	Current Status	Approaches to Fill Gaps
Understanding composition effects on quenched glass chemical durability are limited. Need to determine the mode of radionuclide release and WF degradation. Determine if WF acceptance criteria developed for BS glass WFs are appropriate for iron phosphate WFs. Determine the effect of dissolved phosphate species on solubility limits and transport behaviors of radionuclides used to assess repository performance.	The effects of composition (i.e., O:P molar ratio, Fe:P molar ratio) on quenched glass chemical durability are limited. Tests with developmental DPF materials indicate BS glass WF model is appropriate; Stage 3 behavior not expected.	More work is needed to evaluate the chemical durability of quenched and CCC-treated glasses of varying WLs and compositions. Also, the effects of phosphate on seepage water and chemistry of radionuclides should be studied.

Pacific Northwest National Laboratory

902 Battelle Boulevard
P.O. Box 999
Richland, WA 99354

1-888-375-PNNL (7665)

www.pnnl.gov